Published in : Advanced Healthcare Materials (2024), vol. 13, n°08, pp. 2302712
DOI: 10.1002/adhm.202302712
Status : Postprint (Author's version)

POLY(*N*-METHYL-*N*-VINYLACETAMIDE): A STRONG ALTERNATIVE TO PEG FOR LIPID-BASED NANOCARRIERS DELIVERING SIRNA

Manon Berger, François Toussaint, Sanaa Ben Djemaa, Erik Maquoi, Hélène Pendeville, Brigitte Evrard, Christine Jerôme, Jeanne Leblond Chain, Anna Lechanteur, Denis Mottet, Antoine Debuigne,* and Géraldine Piel**

M. Berger, B. Evrard, A. Lechanteur, G. Piel, Laboratory of Pharmaceutical Technology and Biopharmacy, CIRM, University of Liège, Avenue Hippocrate 15, Liège 4000, Belgium

F.Toussaint, C.Jerôme, A.Debuigne, Center for Education and Research on Macromolecules CERM, CESAM Research Unit, University of Liège, Allée du Six Août, 13, Liège 4000, Belgium

S. Ben Djemaa, D. Mottet, Gene Expression and Cancer Laboratory GEC, GIGA-Molecular Biology of Diseases, University of Liège, Avenue de l'Hôpital 11, Liège 4000, Belgium

E.Maquoi, Laboratory of Tumor and Development Biology, GIGA-Cancer, University of Liège, Avenue Hippocrate, 13, Liège 4000, Belgium

H.Pendeville, Platform Zebrafish Facility and Transgenics, GIGA, University of Liège, Avenue de l'Hôpital, 11, Liège 4000,Belgium

J. Leblond Chain, University of Bordeaux, CNRS, INSERM ARNA, UMR 5320, U1212, 146 rue Léo Saignat, Bordeaux F-33000, France

ABSTRACT

Lipid-based nanocarriers have demonstrated high interest in delivering genetic material, exemplified by the success of Onpattro and COVID-19 vaccines. While PEGylation imparts stealth properties, it hampers cellular uptake and endosomal escape, and may trigger adverse reactions like accelerated blood clearance (ABC) and hypersensitivity reactions (HSR). This work highlights the great potential of amphiphilic poly(N-methyl-N-vinylacetamide) (PNMVA) derivatives as alternatives to lipid-PEG for siRNA delivery. PNMVA compounds with different degrees of polymerization and hydrophobic segments, are synthesized. Among them, DSPE (1,2-distearoyl-sn-glycero-3-phosphoethanolamine)-PNMVA efficiently integrates into lipoplexes and LNP membranes and prevents protein corona formation around these lipid carriers, exhibiting stealth properties comparable to DSPE-PEG. However, unlike DSPE-PEG, DSPE-PNMVA$_{24}$ shows no adverse impact on lipoplexes cell uptake and endosomal escape. In in vivo study with mice, DSPE-PNMVA$_{24}$ lipoplexes demonstrate no liver accumulation, indicating good stealth properties, extended circulation time after a second dose, reduced immunological reaction, and no systemic pro-inflammatory response. Safety of DSPE-PNMVA$_{24}$ is confirmed at the cellular level and in animal models of zebrafish and mice. Overall, DSPE-PNMVA is an advantageous substitute to DSPE-PEG for siRNA delivery, offering comparable stealth and toxicity properties while improving efficacy of the lipid-based carriers by minimizing the dilemma effect and reducing immunological reactions, meaning no ABC or HSR effects.

KEYWORDS :

lipid nanoparticles, lipoplexes, PEG alternative, poly(N-methyl-Nvinylacetamide), siRNA delivery

Published in : Advanced Healthcare Materials (2024), vol. 13, n°08, pp. 2302712
DOI: 10.1002/adhm.202302712
Status : Postprint (Author's version)

1. Introduction

Today, lipid-based nanoparticles represent the predominant non-viral gene therapy technology. In addition to conventional lipoplexes consisting of cationic liposomes complexing siRNA, lipid nanoparticles (LNPs) have emerged as the most advanced group of lipid-based nanoparticles. Indeed, the development of COVID-19 vaccines (Comirnaty and Spikevax) has demonstrated the powerful potential of LNPs and gene (mRNA) delivery for vaccine development. Beyond vaccination, the application of lipid nanovectors, such as LNPs carrying mRNA or siRNA, holds great promise for tackling challenging diseases.[1–4] The FDA approval of Onpattro (patisiran) in 2018 underscores the growing interest in gene delivery within the pharmaceutical research community. Onpattro, the first FDA-approved RNA interference (RNAi) drug, specifically targets the treatment of hereditary ATTR amyloidosis.[5] These recent advances in LNP technology and its applications in gene delivery demonstrate its high potential to treat a wide range of diseases and potentially revolutionize the future of medicine.

Approved LNP formulations have a common composition consisting of four types of lipids: an ionizable lipid, 1,2-distearoylsn-glycero-3-phosphocholine (DSPC), cholesterol and a lipid-polyethylene glycol (lipid-PEG). Instead of cationic lipids used in lipoplex formulations, LNPs incorporate ionizable lipids with pKa value typically below 7, to overcome limitations associated with the use of cationic liposomes (toxicity, low endosomal escape…). The ionizable lipid enables LNPs to be positively charged at acidic pH, facilitating complexation with negatively charged siRNA molecules and promoting interactions with cellular membranes such as those found in endosomes. At physiological pH, LNPs have a neutral charge to prevent unwanted interactions with blood components and the immune system.[1,6]

PEGylation of lipid-based nanoparticles, including lipoplexes and LNPs, is a common strategy to prevent their aggregation and impart stealth properties, thereby prolonging their blood circulating time.[7,8] However, decorating nanoparticles with PEG has drawbacks. Repeated administration of PEG-protected carriers can lead to an increase in anti-PEG IgM and IgG in patients, resulting in adverse immune responses.[9–14] This phenomenon, known as the accelerated blood clearance (ABC) effect, can lead to loss of efficacy, hypersensitivity reactions (HSR) and potentially anaphylactic shock. In addition, PEGylation can lead to drug release problems due to reduced interactions of the carrier with biological membranes of target cells, as well as less efficient endosomal escape, a phenomenon known as the "*PEG dilemma*."[15–21] Despite significant advances in the field of LNPs for mRNA/siRNA delivery, achieving safe and effective delivery to diseased sites remains a major challenge. Therefore, the search for PEG alternatives to avoid potential adverse immunogenic events and to improve the efficacy of lipid-based nanoparticles is as relevant as ever.

Poly(N-vinyl amide)s have gained significant interest in the field of biomedical applications due to their hydrophilicity and biocompatibility. Among these materials, poly(N-vinyl pyrrolidone) (PNVP) is the most widely studied structure.[22–26] In the last years, considerable progress has been made in the design of PNVP, enabling its integration into complex macromolecular structures and its valorization in various cosmetic, pharmaceutical and biomedical applications.[27–30] Recently, some PNVP derivatives have been employed for surface modification of lipid nanocapsules,[31] liposomes,[32–34] and siRNA-loaded lipoplexes.[35] In our recent work, the PNVP-modified lipoplexes showed non-toxicity, prolonged circulation time and, unlike PEG, prevented significant immunogenic effects, thus reducing the ABC effect. However, PNVP did not reduce the *dilemma* effect observed with PEG. Indeed, PNVP-coated lipoplexes showed a similar *dilemma* to PEGylated lipoplexes, as a similar reduction in in vitro efficacy compared to naked lipoplexes was observed.

Published in : Advanced Healthcare Materials (2024), vol. 13, n°08, pp. 2302712
DOI: 10.1002/adhm.202302712
Status : Postprint (Author's version)

Poly(*N*-methyl-*N*-vinylacetamide) (PNMVA) is another poly(*N*vinyl amide) that has been largely disregarded until now in the biomedical field despite its numerous assets. Unlike PNVP, the pendant amide groups of PNMVA are acyclic and composed of one less carbon resulting in greater flexibility and water solubility of the polymer chain. The controlled synthesis of PNMVA and its integration in more complex macromolecular structures were notably achieved by tellurium-mediated radical polymerization,[36] organometallic-mediated radical polymerization[37–39] and very recently by reversible addition fragmentation chain transfer polymerization (RAFT).[40] Compared to the first two approaches, RAFT does not involve any tellurium compounds nor metals whose residues might induce a disqualifying toxicity for biomedical applications.

The present study explores for the first time the use of PNMVA for surface coating of lipid-based nanoparticles, reporting on its advantages as an alternative to PEG and PNVP in the development of stealth and low immunogenic siRNA carriers with enhanced transfection efficiency (**Figure 1**). To enable the anchoring of PNMVA onto the surface of nanoparticles, this polymer was covalently conjugated to hydrophobic groups likely to interact with the lipid-based nanocarriers, namely octadecyl-(OD) and 1,2-distearoyl-sn-glycero-3-phosphoethanolamine (DSPE). The macromolecular parameters and functionalization of PNMVA were precisely controlled through RAFT polymerization.

The resulting amphiphilic PNMVA derivatives were initially tested as decorating agents for siRNA-loaded lipoplexes using a post-modification approach. The cell viability, protein corona formation, immunogenicity, and transfection efficiency of the resulting PNMVA lipoplexes were then examined, highlighting the great potential of PNMVA.

Subsequently, the application of PNMVA was extended to the development of new generation of siRNA-loaded LNPs.[41] To further improve LNP efficiency, a pH-sensitive and switchable lipid, the CSL3 lipid, was used. When the pH within the endosome decreases to an acidic pH, the CSL3 lipid undergoes a conformational change due to the protonation of the central pyridine group. This conformational change triggers the destabilization of lipid nanoparticles and facilitates the complete release of siRNA in less than 15 min.[42]

In summary, this study aims to assess the shielding effect of new hydrophilic PNMVA polymers on both liposome and LNP formulations. Following chemical synthesis, the first part of the study focuses on the surface coverage of lipoplexes, encompassing the evaluation of physicochemical properties of grafted nanocarriers, as well as their in vitro gene efficiency and in vivo safety, immunogenicity and biodistribution in mice. The second part evaluates the potential of these new polymers for LNP modification.

2. Results and Discussion

2.1. SYNTHESIS OF PNMVA DERIVATIVES

The surface modification of lipid-based nanocarriers requires the use of amphiphilic compounds whose hydrophobic part anchors into the lipid membrane and hydrophilic segment decorates the surface of the carrier notably to ensure its stealth properties. In this perspective, the hydrosoluble PNMVA was end-functionalized with two different hydrophobic groups, namely octadecyl (OD) and DSPE (**Figure 2**). OD-PNMVA with low degree of polymerization (DP = 31) and low dispersity ($Đ \approx 1.21$) was obtained via RAFT polymerization of NMVA performed in bulk at 35 °C using an octadecyl-functional xanthate (OD-XA) as chain transfer agent. Well-defined

Published in : Advanced Healthcare Materials (2024), vol. 13, n°08, pp. 2302712
DOI: 10.1002/adhm.202302712
Status : Postprint (Author's version)

DSPE-PNMVA compounds were produced via RAFT of NMVA initiated by a xanthate bearing a succinimidyl carbonate moiety (SC-XA) followed by coupling of the succinimidyl carbonate-PNMVA (SC-PNMVA-XA) with DSPE. The degree of polymerization of PNMVA (DP = 24 or 50) was tuned by adjusting the monomer/RAFT agent molar ratio. Synthesis and characterization of the PNMVA compounds are detailed in the SI (**Scheme S1, Tables S1–S3, Figures S1–S3, Supporting Information**). All polymers were purified by repeated precipitation, dialysis in water and lyophilization. In the case of the DSPE-PNMVA derivatives, the terminal XA removal was achieved by treatment with lauroyl peroxide (LPO) at 80 °C in isopropanol as reported by Destarac et al.[43,44] (**Figure S3, Table S3, Supporting Information**). Proper elimination of the XA terminal group of DSPE-PNMVA was confirmed by the disappearance of the xanthate characteristic absorption peak at 290 mm in the size exclusion chromatography-UV curves (**Figure S3, Supporting Information**). Finally, a low dispersity Et-PNMVA$_{27}$ deprived of long hydrophobic chain was also prepared using ethyl-2((ethoxycarbonothioyl)thio)propanoate (Et-XA) as CTA (**Figure 2**) and will serve as reference.

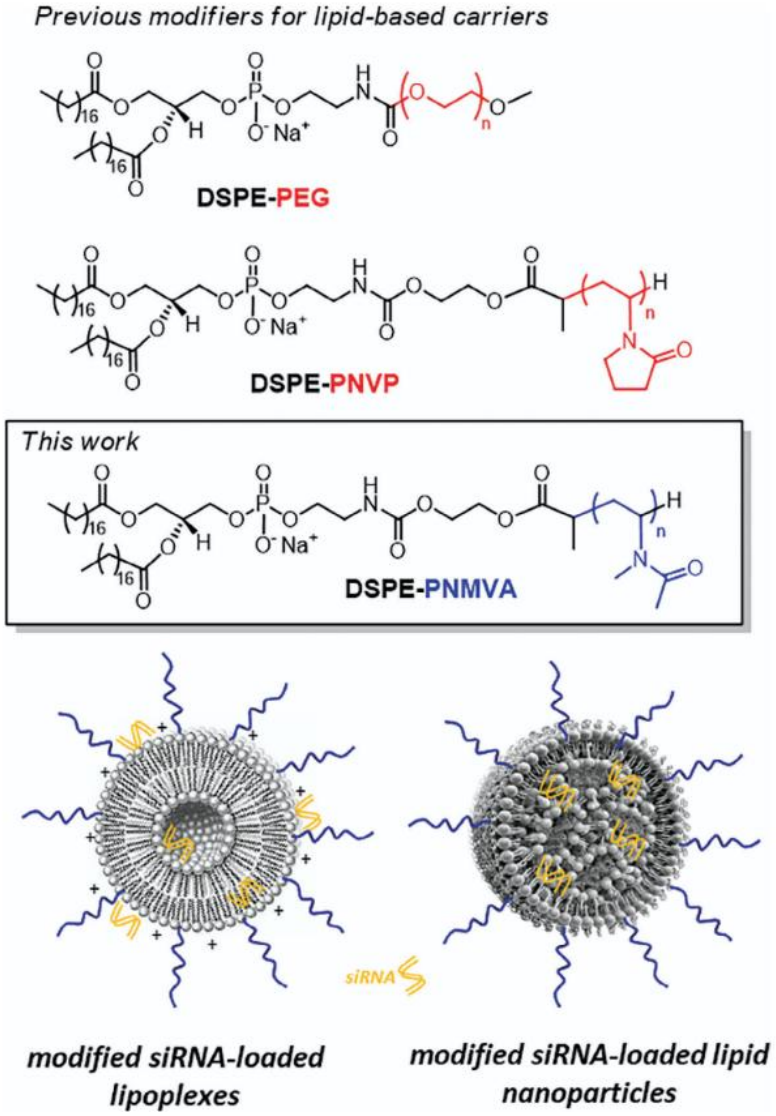

Figure 1. Schematic illustration of the strategy for the PNMVA surface modification of siRNA-loaded lipoplexes and LNPs. Lipid composition: DOTAP/Chol/DOPE 44.4/33.3/22.2 + 15% DSPE-PNMVA molar ratio for lipoplexes; CSL3/DSPC/Chol/DSPE-PNMVA 50/10/37.5/2.5 molar ratio for LNPs.

Published in : Advanced Healthcare Materials (2024), vol. 13, n°08, pp. 2302712
DOI: 10.1002/adhm.202302712
Status : Postprint (Author's version)

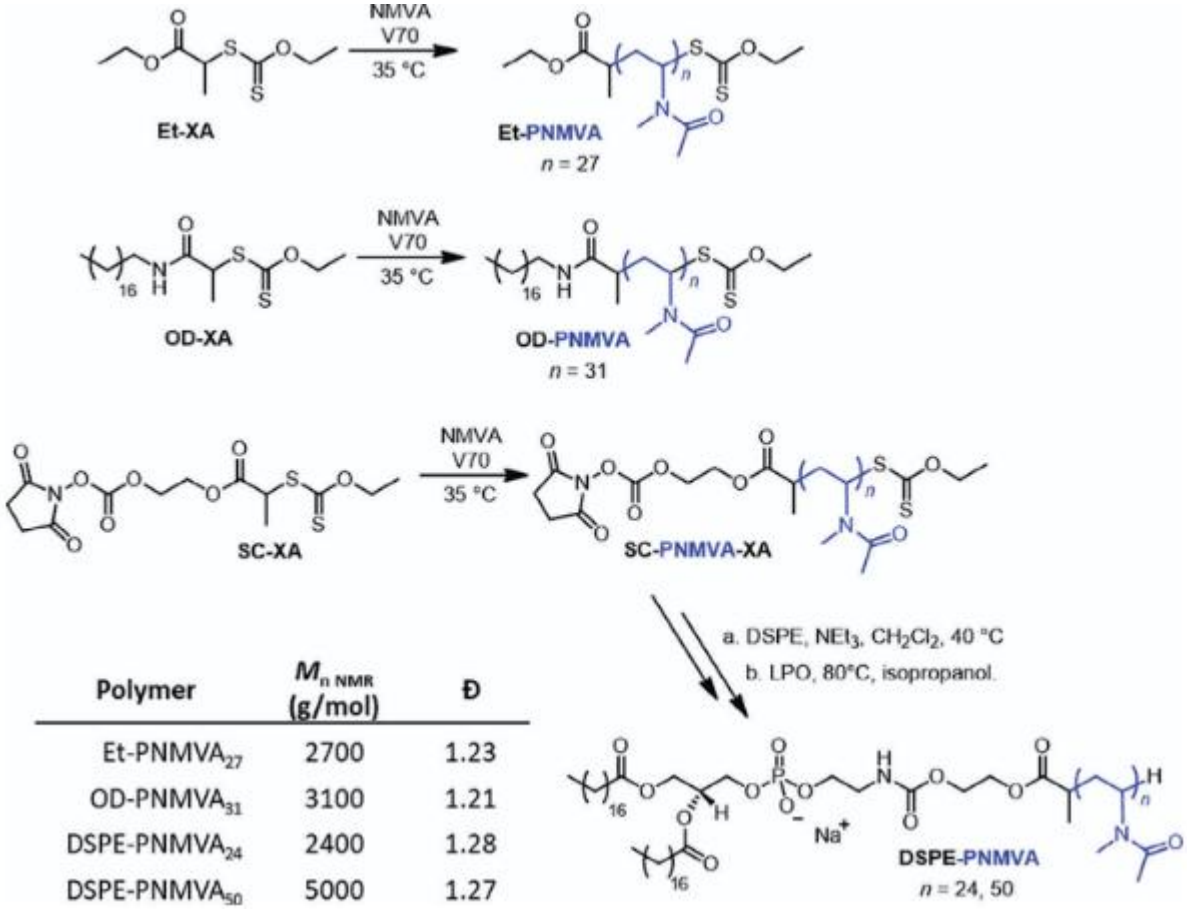

Polymer	$M_{n\ NMR}$ (g/mol)	Đ
Et-PNMVA$_{27}$	2700	1.23
OD-PNMVA$_{31}$	3100	1.21
DSPE-PNMVA$_{24}$	2400	1.28
DSPE-PNMVA$_{50}$	5000	1.27

Figure 2. Synthesis of the amphiphilic PNMVA derivatives.

2.2. INTERACTION OF PNMVA DERIVATIVES WITH LIPID BILAYERS

The capacity of the different PNMVA derivatives to interact with lipid membranes composed of DOTAP/Chol/DOPE (44.44/33.33/22.22 molar ratio) was studied via Quartz Crystal Microbalance with Dissipation (QCM-D) (**Figure 3**). These supported lipid bilayers (SLB) were deposited on gold-coated quartz crystals according to a previously reported procedure[45,46] (**Figure S4, Supporting Information**). The polymer/SBL interaction was monitored by the change in frequency of the QCM-D sensors via the Sauerbrey equation ($\Delta m = -C\,\Delta f/n$, where C is a constant and designates the overtone number).[47,48] As expected, no frequency change was observed when the lipid membrane was exposed to Et-PNMVA$_{27}$, confirming the absence of interaction for PNMVA derivatives deprived of significant hydrophobic group (**Figure3A**). A sharp decrease in frequency ($\Delta f \approx 15$ Hz) was recorded for OD-PNMVA$_{31}$, suggesting its fast interaction with the membrane (**Figure 3B**). However, the frequency re-increased up to $\Delta f \approx 6$–7 Hz upon buffer rinsing, highlighting the weakness of the OD-PNMVA/membrane interactions. A gradual decrease in frequency was observed for both DSPE-PNMVA derivatives (**Figure 3C, D**). For DSPE-PNMVA$_{24}$, the frequency decreased of about 21 Hz. Although a slight mass removal was observed upon rinsing with buffer, most of the DSPE-PNMVA$_{24}$ remained at the membrane's surface as suggested by the stabilization of the frequency around $\Delta f \approx$17–18 Hz (corresponding to a polymer deposition of 45 ng cm^{-2}) (**Figure 3C**). The decrease in frequency was associated with an increase in dissipation ($\Delta D > 0$), which is likely due to a softer and less rigid surface structure induced by the presence of a hydrated PNMVA layer at the surface of the

Published in : Advanced Healthcare Materials (2024), vol. 13, n°08, pp. 2302712
DOI: 10.1002/adhm.202302712
Status : Postprint (Author's version)

membrane (**Figure S5B, Supporting Information**). The frequency versus time curves for the different overtones (fifth to 13th) are very similar which confirms the insertion of the polymer into the membrane rather than its deposition at the surface (**Figure S5A, Supporting Information**).[46] Last, the modification of the SLB by DSPE-PNMVA$_{50}$ led to a lower decrease in frequency (i.e., $\Delta f \approx$5–6 Hz corresponding to Δm≈15 ng cm^{-2}) compared to DSPE-PNMVA$_{24}$ (**Figure 3D**) indicating that DSPE-PNMVA$_{50}$ is too hydrophilic to ensure optimal insertion within the membrane. Overall, best lipid membrane binding was achieved for DSPE-functional PNMVA with DP of about 24 (DSPE-PNMVA$_{24}$).

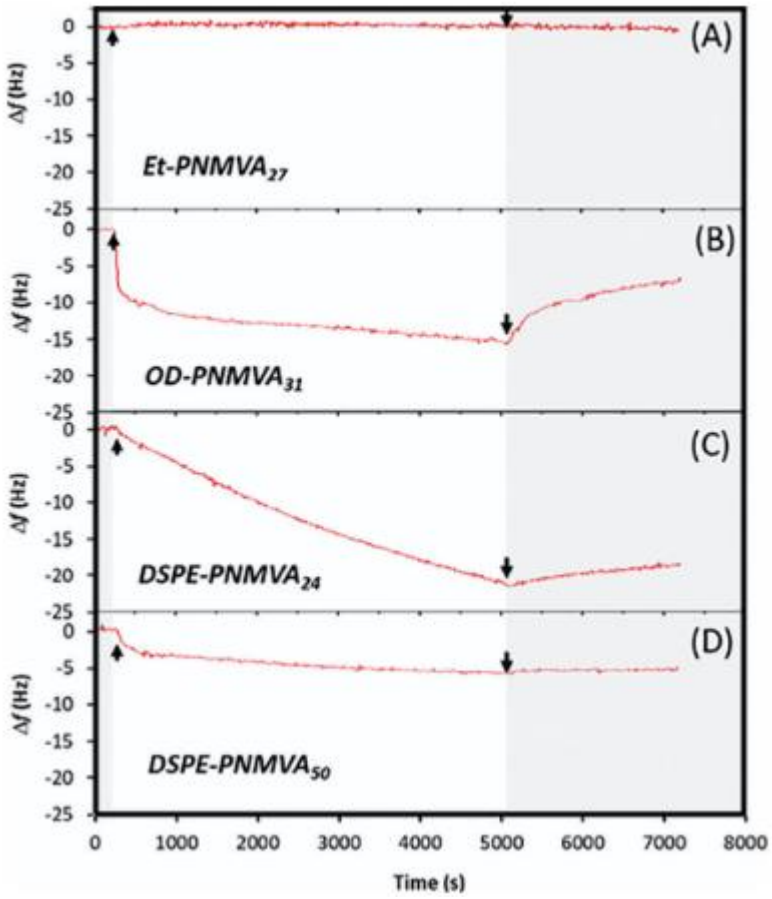

Figure 3. Δf traces (seventh harmonic) from QCM-D monitoring of the deposition of A) Et-PNMVA27 , B) OD-PNMVA31 , C) DSPE-PNMVA24 , and D) DSPE-PNMVA50 at a concentration of 30 µm on DOTAP/Chol/DOPE (37,5/29/18,5 molar ratio) membranes at 25 °C (continuous flow of 30 µm polymer solutions). Arrows designate the polymer solution addition (arrow up) and the final rinsing with buffer (arrow down). Grey regions correspond to buffer elution periods.

Published in : Advanced Healthcare Materials (2024), vol. 13, n°08, pp. 2302712
DOI: 10.1002/adhm.202302712
Status : Postprint (Author's version)

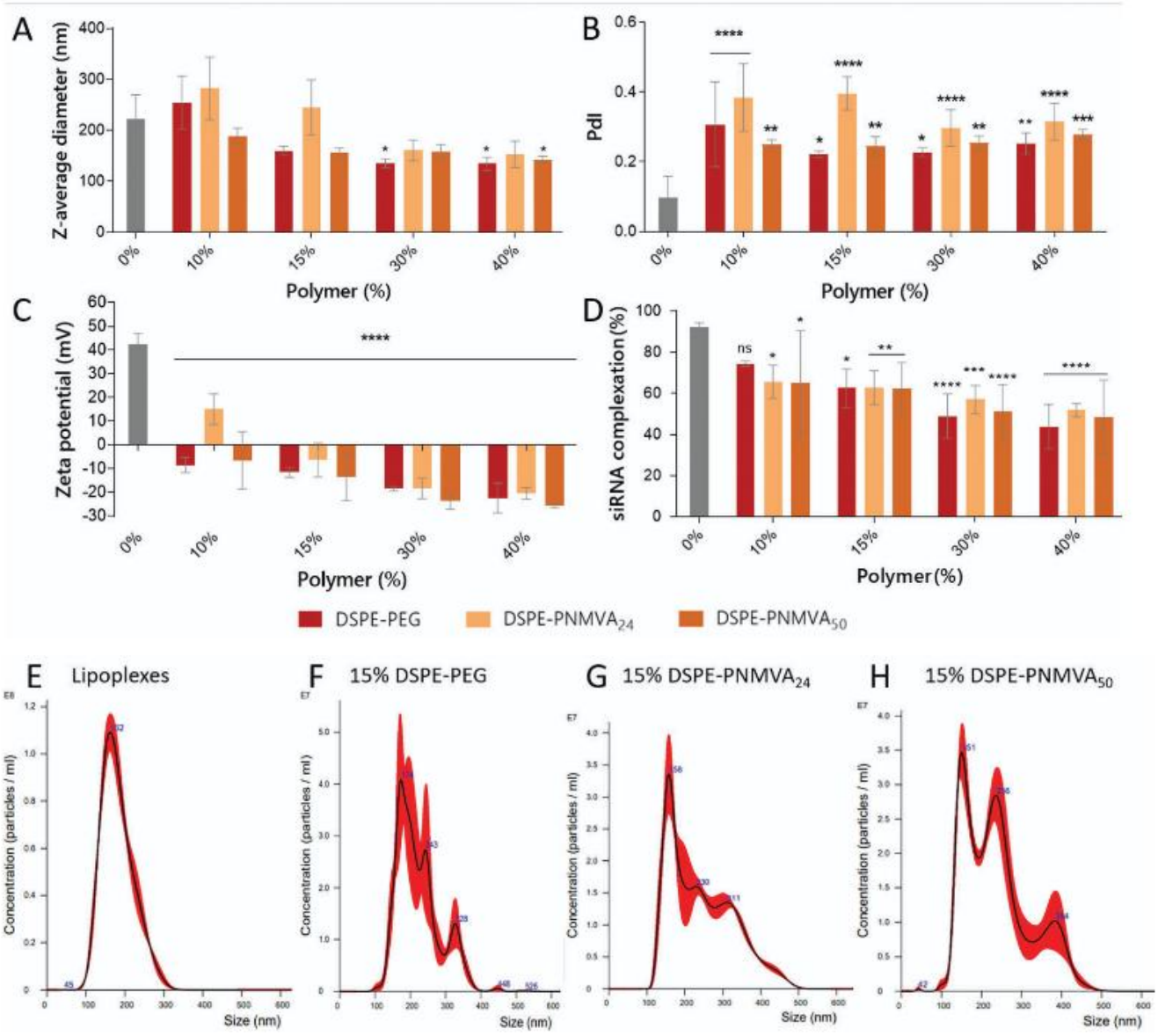

Figure 4. Impact of lipoplexes (N/P 2.5, 100 nm) post-grafting with increasing percentages (0, 10, 15, 30, 40% molar ratio of total lipids) of polymers on physicochemical properties: A) Z-average diameter (nm), B) PdI, C) Zeta Potential (ζ) (mV), and D) siRNA complexation (%). Each value represents the mean +/− standard deviation (SD) of three independent experiments (n = 3). Statistical analyses were performed by one-way ANOVA, followed by the Dunnett's multiple comparisons test where naked lipoplexes were taken as control. The difference between groups was considered significant when the p-value was <0.05 (*), <0.01 (**), <0.001 (***) or <0.0001 (****). D) Particle distribution profiles given by NTA of E) naked lipoplexes or lipoplexes grafted with 15% F) DSPE-PEG, G) DSPE-PNMVA24 , and H) DSPE-PNMVA50 .

2.3. POST INSERTION OF PNMVA DERIVATIVES INTO LIPOPLEXES

2.3.1. Impact of PNMVA Derivatives on Lipoplex Physicochemical Properties

The incorporation of amphiphilic polymers into lipoplexes (DOTAP/Chol/DOPE, 44.44/33.33/22.22 molar ratio, 100 nm siRNA, N/P 2.5) was evaluated by assessing several of their physicochemical properties, including size, polydispersity index (PdI), surface charge (zeta potential ζ) and encapsulation efficiency. Because QCM-D analyses showed that only DSPE derivatives were able to anchor effectively in a lipid bilayer, we focused on these compounds for the surface modification of lipoplexes. The latter were treated with DSPE-PNMVA$_{24}$ and DSPE-

Published in : Advanced Healthcare Materials (2024), vol. 13, n°08, pp. 2302712
DOI: 10.1002/adhm.202302712
Status : Postprint (Author's version)

PNMVA$_{50}$ polymers in different proportions (10%, 15%, 30% and 40% of total lipids, %mol), while DSPE-PEG was used as a positive control at 15%. **Figure 4** shows the properties of the modified lipoplexes and their unmodified counterparts (naked lipoplexes).

The Z-average size of the naked lipoplexes (0%) was ≈200 nm and did not show a significant increase upon addition of different polymers, as shown in **Figure 4A**. However, a decreasing trend in size was observed with increasing polymer concentration. It is worth noting that the addition of polymers had little effect on lipoplex size, except when large amounts of DSPE-PNMVA were added, a trend also observed with DSPE-PEG.

The PdI of the lipoplexes, which was initially below 0.1 for naked lipoplexes, showed a significant increase for DSPE-PNMVA and PEGylated lipoplexes (PdI > 0.2) irrespective of the concentration (**Figure 4B**). The high size dispersity recorded for lipoplexes treated with DSPE polymers highlights their ability to interact with and insert into the lipid-based carriers.

The surface charge (ζ) of all formulations was also evaluated (**Figure 4C**). PEGylation is known to reduce the ζ of cationic liposomes by shielding the positive charges. As expected, all formulations showed a significant decrease in ζ compared to naked lipoplexes, which initially had a charge of ≈+45 mV. At 40%, DSPE-PNMVA lipoplexes exhibited a negative ζ (≈−15 mV), similar to the ζ observed with PEGylated lipoplexes. These results support the idea of efficient polymer insertion around the lipoplexes.

The effect of polymers grafting on siRNA complexation efficiency was evaluated. Naked lipoplexes showed a complexation rate of over 90%, whereas the complexation rate with DSPE-PNMVA lipoplexes decreased to ≈45% in the presence of 40% of these polymers, regardless of the hydrophilic chain length (**Figure 4D**). Interestingly, similar results have been previously reported by our group.[35] Hattori et al. also found an increase in the free fraction of siRNA for PEGylated lipoplexes. The decrease in siRNA complexation could be attributed to the destructuring of the lipid membrane following the insertion of DSPE-based polymers.

This hypothesis was confirmed by NTA analyses, which showed more complex size distribution profiles (particle concentration-size curves) when lipoplexes were decorated with DSPE-PNMVA or DSPE-PEG polymers (15%) (**Figure 4F, H**) compared to naked lipoplexes (**Figure 4E**).

No significant effect of the hydrophilic chain length of the polymers on size, PdI, ζ and encapsulation efficiency (EE) was observed.

2.3.2. Impact of PNMVA Derivatives on the Formation of the Protein Corona around Lipoplexes

In order to evaluate the blood proteins interaction with lipid nanocarrier (protein corona), a nanoparticle tracking method was used following the incubation of decorated-lipoplexes in FBS. After 2 h incubation in heat-inactivated (HI) FBS, lipoplexes were analyzed and compared with native lipoplexes samples. The protein corona formation, which is known to increase the mean particle size, was examined using the NTA technique.

As expected, it was observed that the mean size of naked lipoplexes increased, confirming the presence of a protein corona. **Figure 5A** shows a shift in the size distribution curve toward larger sizes and **Figure 5E** shows the increase in the mean size, which exceeded 100 nm.

Lipoplexes grafted with DSPE-PNMVA and DSPE-PEG showed opposite results. Their size distribution profiles displayed more overlap compared to the initial profile (**Figure 5B–D**) and the size increase was significantly reduced compared to naked lipoplexes (**Figure 5E**). However, a minimum amount of 10% DSPE-PNMVA was

Published in : Advanced Healthcare Materials (2024), vol. 13, n°08, pp. 2302712
DOI: 10.1002/adhm.202302712
Status : Postprint (Author's version)

required to observe a significant difference compared to naked lipoplexes, as observed with PEGylated lipoplexes. These observations confirm the efficacy of both DSPE-PEG and DSPE-PNMVA in preventing the formation of a protein corona around the lipoplexes. A similar study carried out previously confirmed that the increase in particle size after incubation in FBS was not related to the lack of stability of the particles. In this study, we performed control experiments with lipid nanoparticles in water (without serum) during 4 h at 37 °C to exclude that the increase in size could be related to the lack of stability of the particles under the experimental conditions. After 4 h incubation at 37 °C, the particles showed no increase in size and the size distribution profile was not affected by the incubation.[49]

2.3.3. Impact of PNMVA Derivatives on the Lipoplexes Toxicity

Cell viability was assessed using the MTT assay, which measures cellular metabolic activity and serves as an indicator of cell viability, proliferation and cytotoxicity. A549 cells were exposed to naked and modified lipoplexes containing irrelevant GL3 siRNA (siGL3) (**Figure 6**). Cell viability was largely preserved after transfection with naked lipoplexes and lipoplexes decorated with DSPE-PNMVA$_{24}$. In contrast, DSPE-PEG and DSPEPNMVA$_{50}$ lipoplexes showed a significant decrease in cell viability, with ≈50% viability remaining.

The in vivo toxicity of DSPE-PNMVA lipoplexes was evaluated using the zebrafish model, which is widely used to study the in vivo behavior of nanoparticles, including toxicity, biodistribution, pharmacokinetics and therapeutic effects.[50–53] Changes in organ size, shape or effects on embryonic development serve as indicators of biological toxicity. After two consecutive treatments, no specific toxicity was observed compared to the control group up to 72 h post-fertilization (hpf) (**Figure 7**). Zebrafish embryos showed normal morphology at all tested concentrations, with no signs of tail or body axis deformation, pericardial or yolk sac edema or abnormal embryonic development compared to the control group. Based on these findings, it can be concluded that both derivatives of DSPE-PNMVA lipoplexes do not exhibit toxicity to these organisms.

2.3.4. Impact of PNMVA Derivatives on the cell Uptake and Gene Silencing of Lipoplexes

Efficient gene silencing requires successful siRNA internalization and release into the cytoplasm, which are considered as the main critical steps. Because these steps can be limited by PEG (*PEG dilemma*), the impact of PNMVA derivatives on these crucial steps was assessed.

Cellular Uptake Behaviors: First, the cellular uptake of post-grafted lipoplexes formulations was assessed using lipoplexes formulated with fluorescent Cy5-GL3 siRNA (siGL3 Cy 5). **Figure 8A** shows the intracellular fluorescence intensity for DSPE-PEG, DSPE-PNMVA$_{24}$ and DSPE-PNMVA$_{50}$ lipoplexes compared to naked formulations. DSPE-PEG grafting reduced cell internalization of the lipoplexes by ≈80%, which is consistent with the well-known *PEG dilemma*. In contrast, DSPE-PNMVA$_{24}$ and DSPE-PNMVA$_{50}$ lipoplexes exhibited approximately six and threefold higher cellular uptake, respectively, compared to DSPEPEG lipoplexes. This result suggests that these polymers may be less susceptible to the *dilemma* effect. Interestingly, the presence of the DSPE-PNMVA$_{24}$ polymer did not reduce the amount of internalized fluorescent siRNA compared to naked lipoplexes whereas lipoplexes grafted with the DSPE-PNMVA$_{50}$ polymer showed a 50% reduction in cellular penetration, emphasizing the importance to keep the length of the PNMVA low enough to avoid any alteration of cell penetration.

Published in : Advanced Healthcare Materials (2024), vol. 13, n°08, pp. 2302712
DOI: 10.1002/adhm.202302712
Status : Postprint (Author's version)

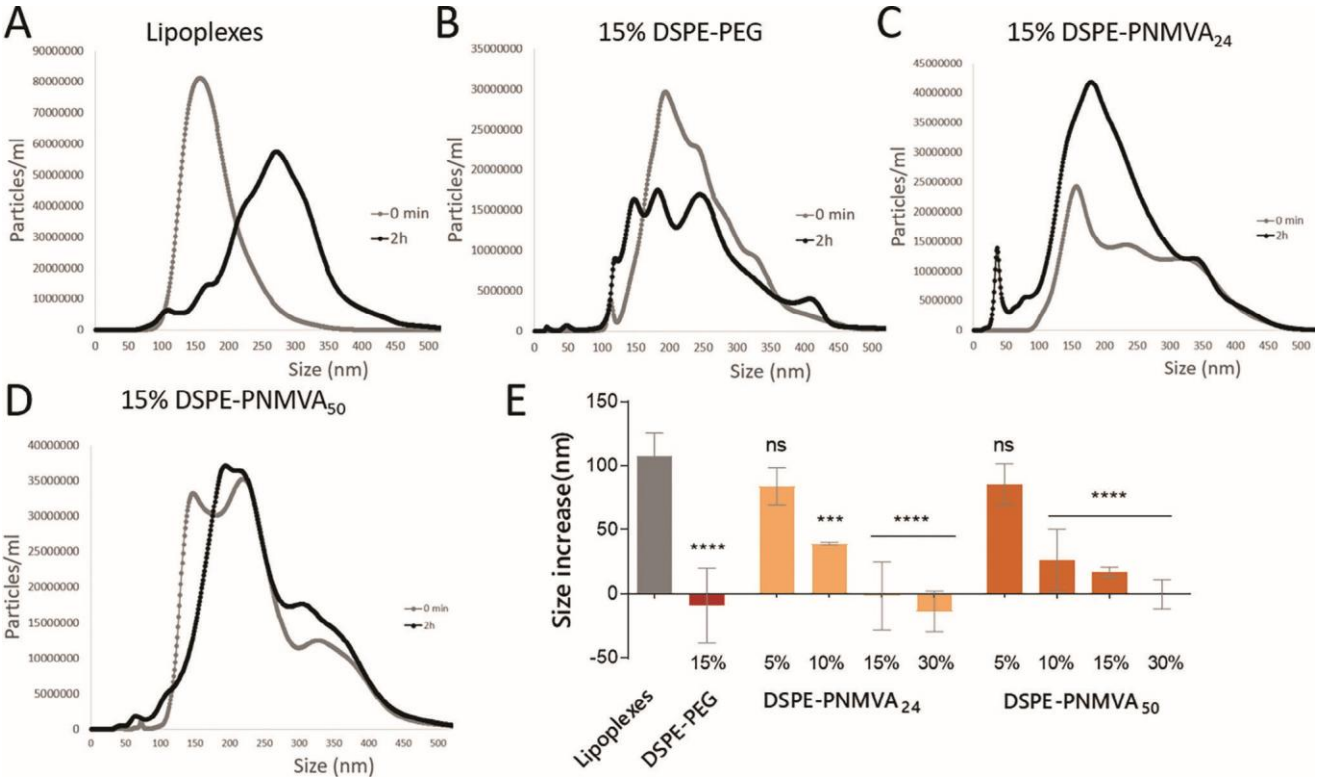

Figure 5. A–D) Particle size (in nm) distribution profiles obtained before and after 2 h of incubation in HI FBS (33.33% v/v) (respectively in grey and black) using the NTA method. E) Increase in the lipoplex mean size after 2 h of incubation in HI FBS (measured using the NTA method). Each value represents the mean +/− standard deviation (SD) of three independent experiments (n = 3). Statistical analyses were performed by one-way ANOVA, followed by the Dunnett's multiple comparisons test where the naked lipoplexes were taken as control. The difference between groups was considered significant when the p-value was <0.05 (*), <0.01 (**), <0.001 (***), or <0.0001 (****).

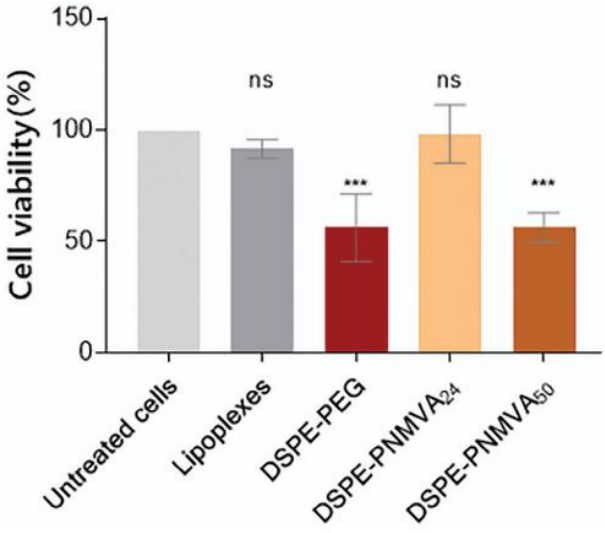

Figure 6. Cell viability of A549 cell line treated for 24 h with lipoplexes or grafted lipoplexes (15%) determined using MTT cell viability assay. Statistical analyses were performed using a one-way ANOVA test, where results were compared to untreated cells. The difference between groups was considered significant when the p-value was <0.05 (*), <0.01 (**), <0.001 (***) or <0.0001 (****).

Gene Silencing Efficiency: As lower uptake might be associated with lower efficiency, we next evaluated the effect of polymers on the gene silencing efficiency of lipoplexes. For this purpose, we used A549 cells stably expressing GFP (A549/GFP cells) as an in vitro cellular model. These cells were transfected with naked and grafted

Published in : Advanced Healthcare Materials (2024), vol. 13, n°08, pp. 2302712
DOI: 10.1002/adhm.202302712
Status : Postprint (Author's version)

lipoplexes carrying a siRNA directed against GFP (siGFP). The decrease in GFP fluorescence intensity, measured by FACS, is used as an indicator of siRNA transfection efficiency, combining cellular uptake, delivery/release and degradation of the target GFP mRNA. Our results showed that naked lipoplexes reduced fluorescence by ≈60% after 72 h of transfection. Consistent with the *PEG dilemma*, PEGylated lipoplexes showed a smaller decrease in GFP fluorescence (≈40%). As a reminder, a limited reduction in fluorescence of only 40% was also observed for the previously investigated DSPE-PNVP lipoplexes.[35] DSPE-PNMVA$_{50}$ lipoplexes showed a similar GFP fluorescence decrease (40%) as DSPE-PEG lipoplexes (Figure 8B). Interestingly, 15% DSPE-PNMVA$_{24}$ lipoplexes appeared to be the most efficient in reducing GFP fluorescence intensity, achieving a reduction of up to 65%.

The better efficiency of the DSPE-PNMVA$_{24}$ lipoplexes appears to correlate with their enhanced cellular uptake as observed in **Figure 8A**. Although the difference is not statistically significant, these results suggest that increasing the hydrophilic chain length of DSPE-PNMVA tends to decrease their efficiency. Furthermore, with regard to the effect of polymer percentage, the best polymer concentration appears to be 15%. Indeed, higher percentages do not further improve the efficiency. Overall, the results show a better efficiency and a less pronounced *dilemma* effect of DSPE-PNMVA$_{24}$ compared to DSPE-PEG and DSPE-PNVP.[35]

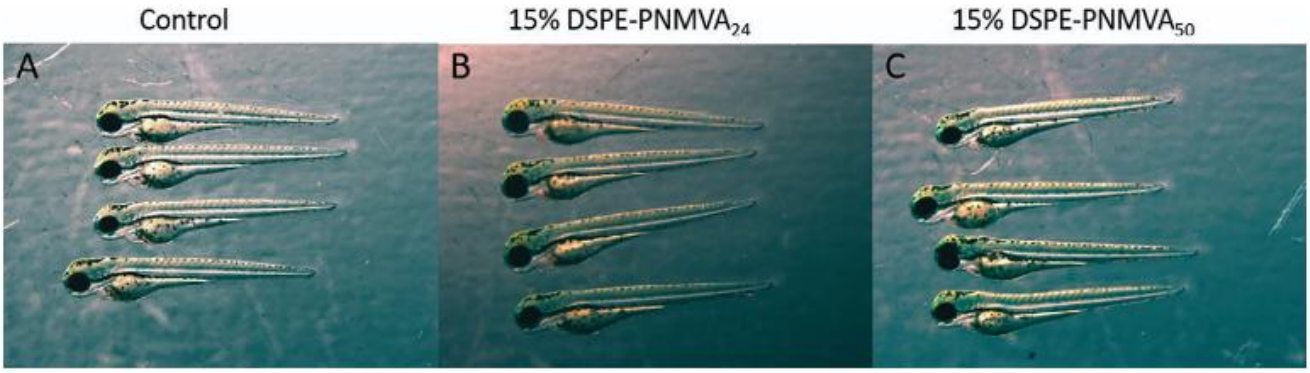

Figure 7. Assessment of lipoplex (100 nm siGL3) toxicity in Zebrafish model after 2 administrations at 10 g siRNA/kg (72 hpf) compared with control condition. A) Control, B) DSPE-PNMVA$_{24}$ lipoplexes, and C) DSPE-PNMVA$_{50}$ lipoplexes. Results showing the assessment of toxicity after the administration of naked lipoplexes and PEGylated lipoplexes have been published previously.[35]

2.3.5. In vivo Evaluation of PNMVA Lipoplexes in Mice

DSPE-PNMVA$_{24}$ lipoplexes (15%) showed promising properties including i) compatible physicochemical characteristics, ii) safety in vitro and in vivo, iii) high internalization and gene silencing efficiency. This lipoplex formulation seems to be a promising alternative to PEG and we have further evaluated its in vivo behavior and compared it to DSPE-PEG.

Biodistribution and ABC Effect: The biodistribution and stealth properties of DSPE-PNMVA$_{24}$ and DSPE-PEG lipoplexes coupled with fluorescent siGL3 Cy 5.5 were assessed in immunocompetent BALB/c mice following two intravenous injections (once a week). The fluorescence intensity of lipoplexes was monitored 5 h and 24 h post-injection using an in vivo imaging system. Following the first injection, similar fluorescence intensity was detected in mice 5 h after injection for both formulations (**Figure 9A and Figure S6, Supporting Information**). This fluorescence intensity decreased 24 h post-injection. After the second injection, the fluorescence observed 5 h later tends to be almost similar to that observed after the first injection. 24 h after the second injection, a weak but significant fluorescent signal was detected in mice injected with DSPE-PEG and DSPE-PNMVA$_{24}$ lipoplexes

Published in : Advanced Healthcare Materials (2024), vol. 13, n°08, pp. 2302712
DOI: 10.1002/adhm.202302712
Status : Postprint (Author's version)

compared to the negative control (mice injected with PBS) (**Figure 9A and Figure S6, Supporting Information**). This result shows that these lipoplexes exhibit an extended circulation time after the second injection, suggesting a reduced ABC effect for these nanoparticles.

To further investigate the biodistribution of DSPE-PNMVA$_{24}$ lipoplexes, a post-mortem analysis of the fluorescence was performed on organs including the liver, spleen, heart, lung, and kidney. No fluorescence was detected in organs such as the liver, lung, and spleen. The absence of hepatic accumulation of lipoplexes confirms their stealthiness and suggests that they are not cleared by the MPS (mononuclear phagocyte system). However, a significant fluorescent signal was detected in the kidney and heart for both DSPE-PEG and DSPE-PNMVA$_{24}$ lipoplexes (Figure 9B). The fluorescence intensity observed in the kidney suggests that these formulations are likely eliminated by the renal route. The accumulation of DSPE-PEG and DSPE-PNMVA$_{24}$ lipoplexes in the kidney is likely due to a combination of various physicochemical characteristics such as size, ζ, shape and composition.

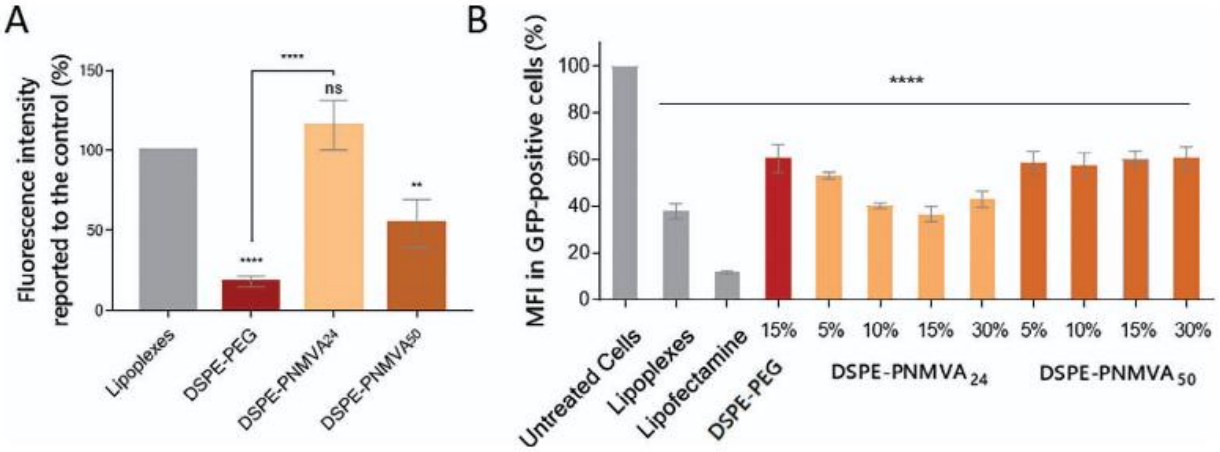

Figure 8. Effect of PNMVA derivatives on A) Cellular uptake of lipoplexes and grafted lipoplexes (15% polymer) in A549 cells. Intracellular fluorescence intensity of siGL3 Cy 5 was detected by flow cytometry after 4 h of incubation. Each value represents the mean +/− standard deviation (SD) of three independent experiments (n = 3). Statistical analyses were performed using a one-way ANOVA followed by the Dunnett's multiple comparisons test where the naked lipoplexes were taken as control. B) Gene knockdown (MFI, %) in A549/GFP cells when transfected with lipoplexes carrying siGFP (100 nm) compared with naked lipoplexes, lipoplexes grafted with DSPE-PEG, and Lipofectamine RNAiMAX after 72 h of transfection (n = 3). Statistical comparisons with untreated cells were performed by one-way ANOVA, followed by the Dunnett's multiple comparisons test. The difference between groups was considered significant when the p-value was <0.05 (*), <0.01 (**), <0.001 (***) or <0.0001 (****).

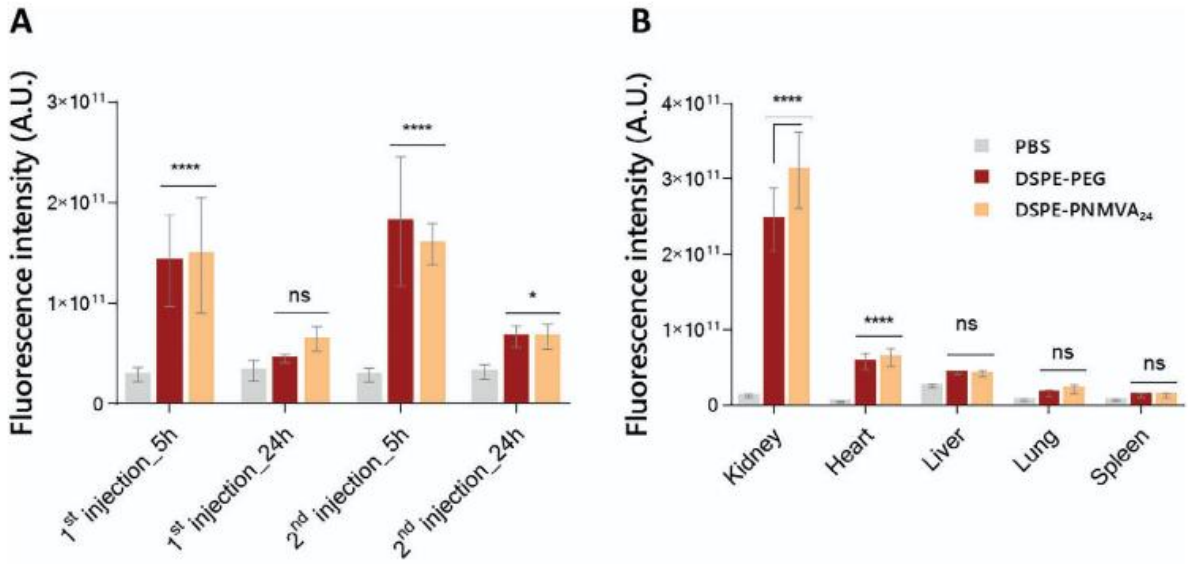

Published in : Advanced Healthcare Materials (2024), vol. 13, n°08, pp. 2302712
DOI: 10.1002/adhm.202302712
Status : Postprint (Author's version)

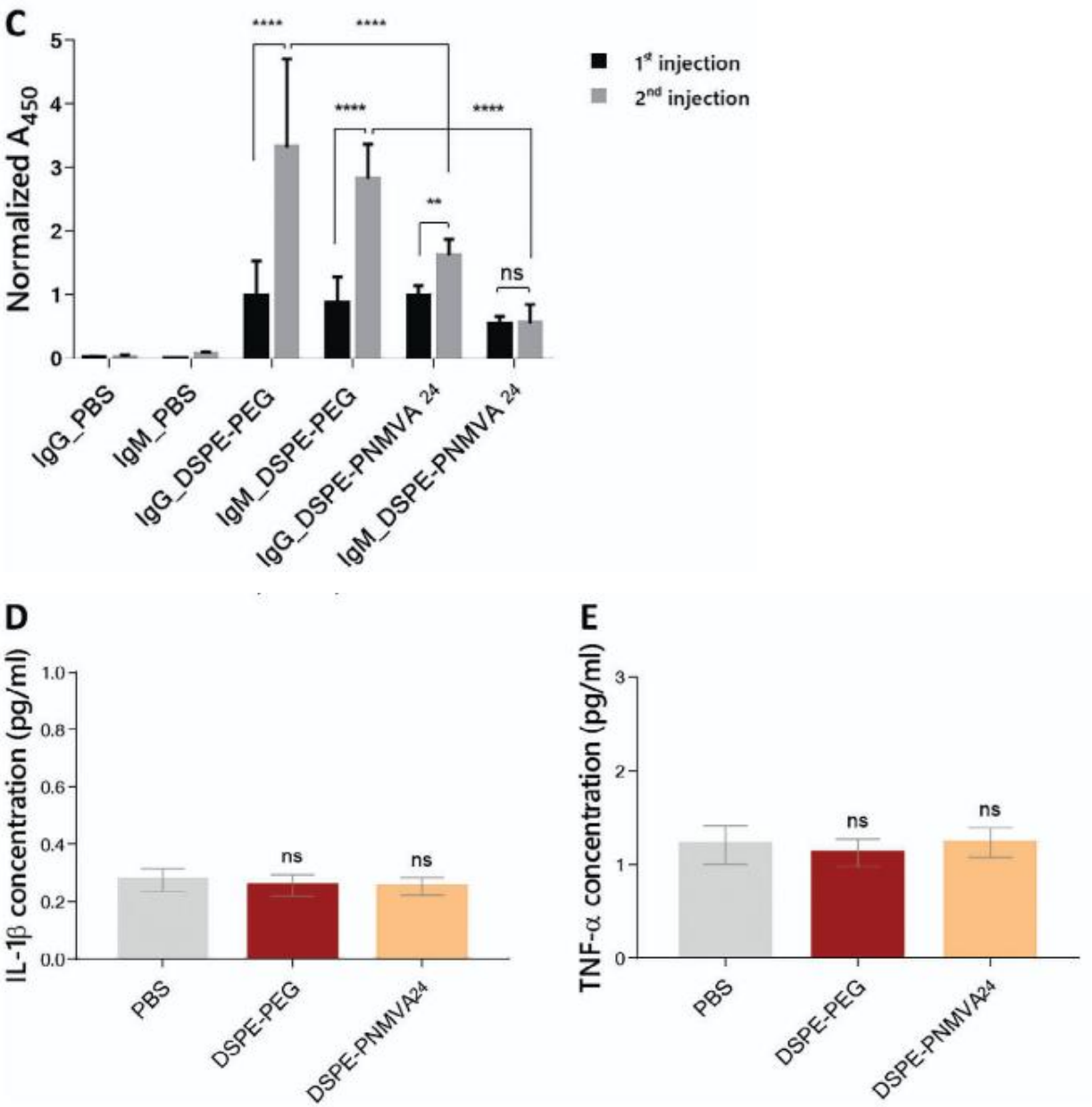

Figure 9. A) Biodistribution of DSPE-PEG and DSPE-PNMVA$_{24}$ lipoplexes detected using in vivo imaging. In vivo fluorescence intensity was measured after 5 and 24 h of the first and the second intravenous injection. B) The body accumulation of DSPE-PEG and DSPE-PNMVA$_{24}$ lipoplexes prepared with siGL3 Cy 5.5 was detected by measuring the fluorescence intensity using ex vivo fluorescence imaging in kidney, heart, liver, lung and spleen. C) The evolution of IgM and IgG production in mice was detected using ELISA assay 1 week after the first and the second injection of DSPE-PEG lipoplexes and DSPE-PNMVA$_{24}$ lipoplexes. Immune-mediated toxicity was assessed by measuring detecting the production of D) IL-1β and E) TNF-α in the serum of mice 1 week after the second injection using ELISA assay. Results were compared to a negative control group injected with PBS. Each value represents the mean +/− standard deviation (SD) of at least 7 mice (n = 7 or 8). For ELISA assay, the result of each mouse represents the mean of a duplicate. Statistical analyses were performed by two-way ANOVA test. The difference between groups was considered significant when the p-value was <0.05 (*), <0.01 (**), <0.001 (***), or <0.0001 (****).

Published in : Advanced Healthcare Materials (2024), vol. 13, n°08, pp. 2302712
DOI: 10.1002/adhm.202302712
Status : Postprint (Author's version)

Immune Response: Assessment of IgM and IgG Production and Proinflammatory Cytokines: To evaluate whether PNMVA could also elicit an immune response and potentially induce inflammation-mediated toxicity, we measured soluble immune mediators, including IgG and IgM antibodies, as well as proinflammatory cytokines.

IgM are produced after the first exposure to an antigen and are then rapidly replaced by IgG, which represents a later-stage response and ensures long-term immune response. The levels of IgM and IgG specific to DSPE-PEG or DSPE-PNMVA$_{24}$ were evaluated in the serum of mice 1 week after each injection using ELISA assay (**Figures 9C**).

For DSPE-PEG lipoplexes, the production of both IgG and IgM was observed after the first injection (**Figure 9C**). After the second injection, the levels of anti-DSPE-PEG IgM and IgG further increase, exhibiting approximately a threefold induction compared to the first injection. This higher presence of detectable anti-PEG IgG after the second injection suggests the development of immunological memory. This rapid elevation of anti-PEG antibody levels upon repeated lipoplex injections could pose significant challenges, potentially leading to severe adverse reactions.

Concerning the DSPE-PNMVA$_{24}$ lipoplexes (**Figure 9C**), we also observed the accumulation of both anti-PNMVA$_{24}$ IgM and IgG after the first injection, suggesting that the first administration stimulates responses by host immune system. However, after the second injection of DSPE-PNMVA$_{24}$ lipoplexes, no increase in anti-DSPE-PNMVA$_{24}$ IgM was detected compared to the first injection. A slight increase in anti-DSPE-PNMVA$_{24}$ IgG was observed after the second administration, representing approximatively a 1.5-fold induction compared to the first injection. However, this increase in IgG anti-DSPE-PNMVA$_{24}$ was lower than the increase observed for anti-DSPE-PEG IgG (threefold induction). These results suggest that DSPE-PNMVA$_{24}$ lipoplexes induce a weaker immune memory response and are therefore less immunogenic than DSPE-PEG lipoplexes.

To evaluate the immunotoxicity of DSPE-PEG or DSPEPNMVA$_{24}$ lipoplexes, we finally measured the production of the two most common pro-inflammatory cytokines (TNF-α, IL-1β) after two intravenous injections by ELISA. The levels of IL-1β and TNF-α in the serum of mice injected with grafted lipoplexes were comparable to the PBS control group (**Figure 9D, E**). This indicates that the intravenous administration of these grafted lipoplexes did not induce systemic inflammation-related responses and did not show immunotoxicity in mice. In accordance with the lack of toxicity in vitro and in in vivo zebrafish model, these results further confirmed the safety of DSPE-PNMVA$_{24}$ lipoplexes for in vivo applications.

2.4. INSERTION OF PNMVA DERIVATIVES INTO SIRNA-LNPS

To broaden the scope of PNMVA derivatives, the incorporation of DSPE-PNMVA$_{24}$ into an innovative LNP formulation was evaluated. The formulation is composed of CSL3/DSPC/Chol/DSPEPEG in a molar ratio 50/10/37.5/2.5 and has demonstrated its ability to effectively decrease mEmerald fluorescence inhibition on MDA-MB-23159 tumor cells.[49] LNPs of similar composition have been prepared but DSPE-PEG has been substituted by DSPE-PNMVA. The properties and performance of the modified LNPs were then evaluated. Compared to the previous formulation of lipoplexes, LNPs were prepared by rapid mixing, which allows pre-insertion of DSPE-PEG and DSPE-PNMVA instead of post-insertion.

Published in : Advanced Healthcare Materials (2024), vol. 13, n°08, pp. 2302712
DOI: 10.1002/adhm.202302712
Status : Postprint (Author's version)

As it is not possible to produce non-PEGylated LNPs by the rapid mixing method, naked lipoplexes could not be used as a control in these studies.

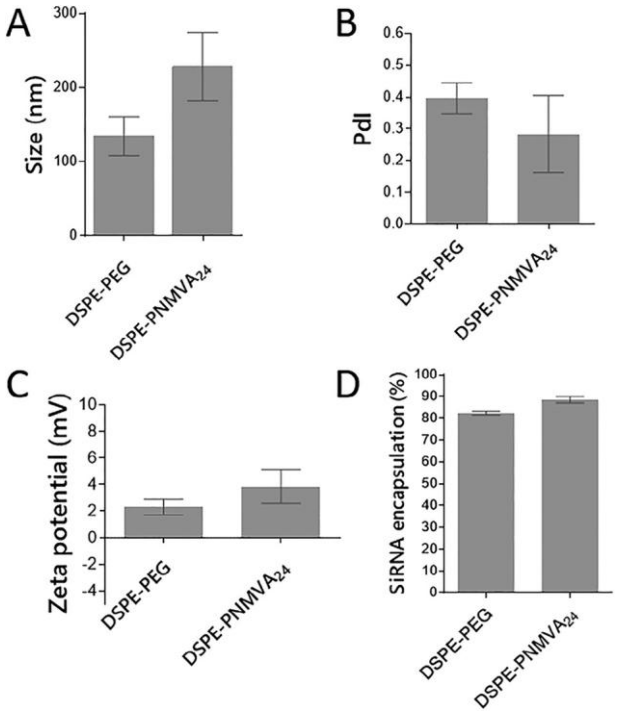

Figure 10. Physicochemical characterization of CSL3 LNPs including DSPE-PEG or DSPE-PNMVA$_{24}$ at 2.5% A) Z-Average obtained using DLS, B) PdI, C) Zeta potential (ζ) obtained by the DLS method and D) siRNA encapsulation efficiency (%) measured using the Quant-iT RiboGreen RNA assay (n = 3).

2.4.1. Impact of PNMVA Derivatives on size, Polydispersity and Surface Charge of LNPs

According to the results shown in **Figure 10A**, the size of DSPE-PNMVA$_{24}$ LNPs were larger than the DSPE-PEG LNPs (228 nm and 135 nm respectively). A further optimization of the LNP production method could probably help to decrease the mean size. Surface charge (ζ) analysis, shown in **Figure 10B**, indicated that both DSPE-PEG and DSPE-PNMVA$_{24}$ LNPs exhibited a neutral ζ, consistent with the expected properties of LNPs at physiological pH. Moreover, the EE of siRNA was high for both DSPE-PEG and DSPE-PNMVA$_{24}$ LNPs, with ≈80% efficiency, as shown in Figure 10C. These results tend to confirm the successful incorporation of the DSPE-PNMVA into LNPs.

2.4.2. Impact of PNMVA Derivatives on the Formation of the Protein Corona around LNPs

LNPs were analyzed by NTA before and after incubation in complete FBS to evaluate the capacity of PNMVA to protect LNP from the formation of the protein corona. The results, shown in **Figure 11**, show a decrease or slight change in mean size combined with an increase in total particle concentration. In line with previous results obtained with lipoplexes and other studies carried out by our group, the formation of protein corona around the nanoparticles generally leads to an increase in particle size and/or a decrease in concentration.[49] These results were correlated with the non-

Published in : Advanced Healthcare Materials (2024), vol. 13, n°08, pp. 2302712
DOI: 10.1002/adhm.202302712
Status : Postprint (Author's version)

adsorption of serum particles onto LNPs, resulting in the observed increase in particle concentration after 2 h of incubation. This concentration includes both free serum particles and LNPs. The decrease in total mean particle size observed in the DSPE-PNMVA$_{24}$ LNP sample was consistent with the absence of adsorption of serum particles onto the LNPs. Indeed, serum particles that are not adsorbed onto the LNPs are free and are tracked by the NTA as well. When analyzed alone, serum particles showed a mean size smaller (121 nm) than what is measured with DSPE-PNMVA$_{24}$ LNPs (190 nm) before the incubation. Hence, when the DSPE-PNMVA$_{24}$ LNPs are incubated in FBS, non-adsorbed serum particles tend to decrease the total particle mean size. This result confirms the ability of DSPEPNMVA$_{24}$ to limit protein corona formation, similarly to DSPEPEG, with the promise of excellent stealth properties. It should also be noted that when DSPE-PNMVA$_{24}$ is used for pre-insertion in LNP formulations, a lower percentage of polymer helps to protect against protein corona formation. Specifically, while a minimum of 15% DSPE-PNMVA$_{24}$ was required in the lipoplexes formulation, only 2.5% appears to be sufficient in the LNP formulation.

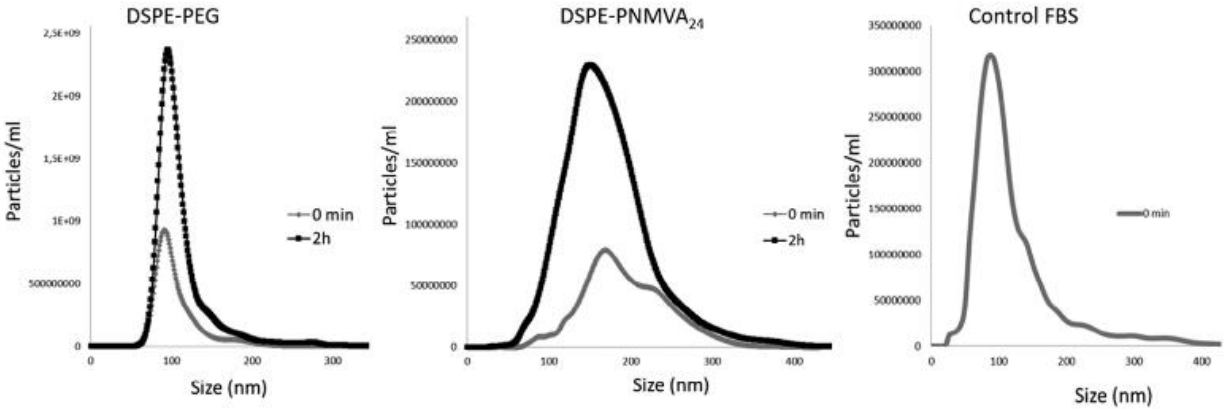

Figure 11. Particle distribution profiles (concentration–size curves) given by the NTA during CSL3 LNPs incubation at 37 °C in serum (FBS) over time, and control complete FBS.

2.4.3. Impact of PNMVA Derivatives on LNP gene Silencing Efficacy

LNPs (100 nm siGFP) containing either DSPE-PEG or DSPE-PNMVA$_{24}$ were evaluated for their ability to deliver siRNA into A549/GFP cells. During the transfection period, cellular fluorescence intensity was analyzed using live cell imaging. This approach provided results comparable to those obtained by FACS after transfection of cells with similar LNP formulations (data not shown). However, live cell imaging allowed a kinetic monitoring of fluorescence inhibition over a 72-h period, contrasting with FACS analysis that is used at a single end point 72 h after transfection.

After 72 h, DSPE-PEG LNPs demonstrated efficient inhibition of GFP fluorescence, resulting in over 65% inhibition. However, this inhibitory effect was reduced when transfection was performed in the presence of serum, resulting in less than 45% fluorescence inhibition (**Figures 12A and 13**).

In contrast, LNPs containing DSPE-PNMVA$_{24}$ polymer showed a remarkably high level of fluorescence inhibition, comparable to that achieved with Lipofectamine, used as a positive control. The inhibition

Published in : Advanced Healthcare Materials (2024), vol. 13, n°08, pp. 2302712
DOI: 10.1002/adhm.202302712
Status : Postprint (Author's version)

of GFP fluorescence exceeded 80%, as shown in **Figure 12A**. Importantly, this high inhibition was maintained even in the presence of serum, distinguish it from PEGylated LNPs. These results could then confirm the superior efficiency of pH-sensitive LNPs produced by rapid mixing.

These findings suggest that DSPE-PNMVA$_{24}$ may not act as a barrier to gene delivery when used in either lipoplex or LNP formulations, avoiding the *dilemma* previously observed with PEG and PNVP derivatives.

Finally, as shown in **Figure 12B** and **Figure 13**, the tested LNPs (100 nm siGL3) demonstrated no significant impact on cell metabolic activity, after 72 h of transfection, and when compared to untreated cells. These results were correlated with previous works showing the safe use of CSL3 lipid,[49] but also with this work that demonstrated the safe use of DSPE-PNMVA derivatives.

3. Conclusion

Innovative amphiphilic polymers composed of PNMVA and hydrophobic OD- or DSPE- segments were synthesized via up-to-date controlled polymerization techniques with the aim to replace PEG for the surface modification of lipoplexes and LNPs dedicated to efficient siRNA delivery combined with good stealth properties and reduced immune response.

Based on physicochemical properties(size, PdI, surface charge (ζ), EE) and efficiency in reducing protein corona formation, we observed that DSPE-PNMVA polymers can be efficiently grafted into lipoplexes and LNP formulations, as is the case for DSPEPEG.

We also evidenced that incorporation of 15% DSPE-PNMVA$_{24}$ strongly limits the formation of a protein corona around lipoplexes, suggesting good stealth properties comparable to those obtained with 15% DSPE-PEG. Moreover, a concentration of 2.5% DSPE-PNMVA$_{24}$ was sufficient to prevent interaction of LNP with blood proteins. This may be explained by the different modes of insertion of DSPE-PNMVA. Pre-insertion into LNPs seems to be more effective than the post-insertion technique used for lipoplexes.

Compared to naked lipoplexes, we observed that insertion of 15% DSPE-PNMVA$_{24}$ polymer had no effect on cell uptake of lipoplexes, unlike what was observed with DSPE-PEG and DSPE-PNVP polymers. This was confirmed by the efficiency of GFP gene silencing, with DSPE-PNMVA$_{24}$ lipoplexes providing 65% fluorescence silencing, whereas DSPE-PEG lipoplexes reduced fluorescence by 40%. It is important to note that a limited fluorescence reduction of 40% was previously observed with DSPE-PNVP$_{30}$ polymers[35] highlighting the interest of this new grafting-polymer.

In contrast to DSPE-PEG, DSPE-PNMVA presents an ester bond in the linker between the lipid and the polymer. The question of the in vivo stability of this ester bond and on its possible role in the observed enhanced internalization for DSPE-PNMVA is relevant. Even if it was not possible to monitor the in vivo stability of the DSPE-PNMVA ester bond, especially at the surface of the nanocarrier, several observations lead us to believe that the ester link remains stable under in vivo conditions. First, the NTA assays show the stability of lipoplexes/LNP-PNMVA comparable to that of lipoplexes/LNP-PEG formulations in the presence of 33% serum. If the ester bond had been cleaved, we would have recovered an NTA profile comparable to that of naked lipoplexes. Second, the previously reported

Published in : Advanced Healthcare Materials (2024), vol. 13, n°08, pp. 2302712
DOI: 10.1002/adhm.202302712
Status : Postprint (Author's version)

DSPE-PNVP[35] having the same ester-based linker showed limited gene silencing efficiency (reduction of the fluorescence by 40%) as DSPE-PEG (reduction of the fluorescence by 40%) and lower efficiency compared to DSPE-PNMVA (offering a reduction of the fluorescence by 65%). These observations support the hypothesis that the high efficiency/internalization recorded for DSPE-PNMVA does not exclusively rely on the linker structure and emphasizes the key role of the nature of the polymer structure used for the decoration of the lipid-based carriers.

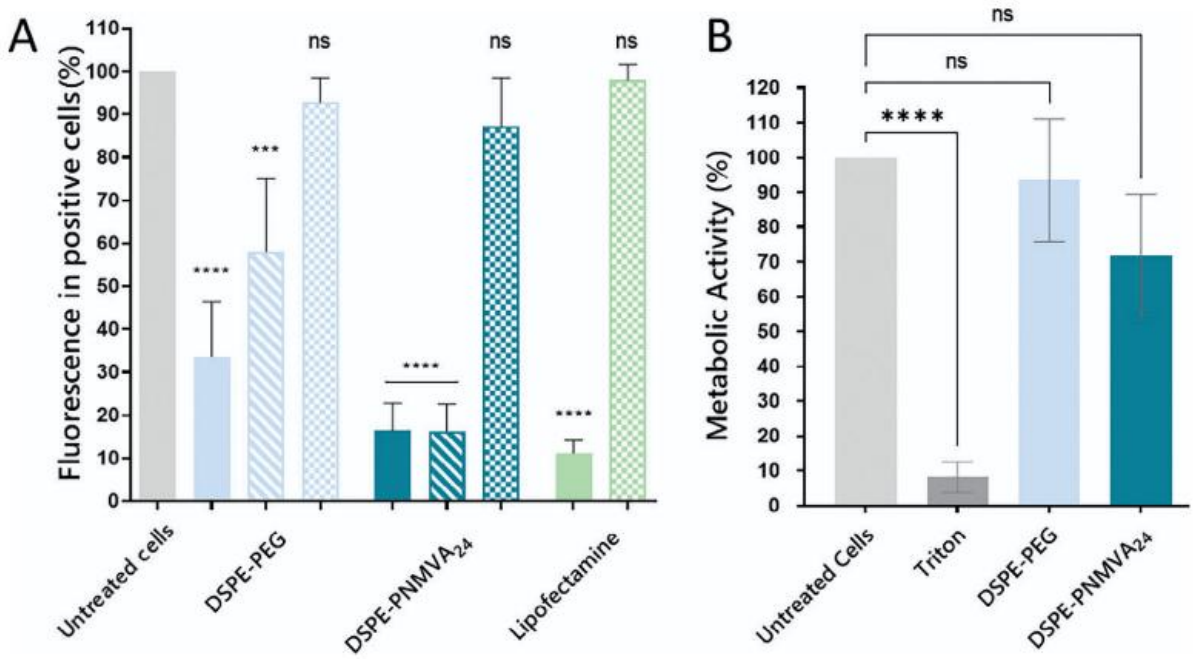

Figure 12. A) Fluorescence in positive A549 cells (%) transfected with CSL3 LNPs (100 nm siGFP) including DSPE-PEG or DSPE-PNMVA 24 and with Lipofectamine, after 72 h of transfection in serum-free medium (filled bars) and in medium containing 10% FBS (hatched bars). LNPs and Lipofectamine with 100 nm siGL3 were also used as negative control (patterned bars). B) Impact of LNPs on in vitro metabolic activity using Resazurin, 72 h post-transfection. Each value represents the mean +/− standard deviation (SD) of three independent experiments (n = 3). Statistical analyses were performed by One-way ANOVA followed by the Dunnett's multiple comparisons test where the untreated cells were taken as control. The difference between groups was considered significant when the p-value was <0.05 (*), <0.01 (**), <0.001 (***), or <0.0001 (****).

In vivo study in mice showed the absence of liver accumulation and thus, prolonged circulation time and good stealth properties of DSPE-PNMVA$_{24}$ lipoplexes which also highlights the stability of the ester linker of DSPE-PNMVA and the stability of the polymer shell around the nanocarrier. An extended circulation time 24 h after a second dose injection was observed likely due to a decreased ABC phenomenon compared to DSPEPEG lipoplexes. Moreover, after the second injection of DSPEPNMVA$_{24}$ lipoplexes, a slight significant increase (≈1.5-fold) was observed for anti-DSPE-PNMVA$_{24}$ IgG, but no increase of antiDSPE-PNMVA$_{24}$ IgM was detected, compared to the first injection. In contrast, the levels of anti-DSPE-PEG IgM and IgG increased by about threefold compared with the first injection. Furthermore, no systemic pro-inflammatory response was observed for DSPE-PNMVA$_{24}$ lipoplexes.

Importantly, our results demonstrated the safety use of PNMVA$_{24}$ polymers in *in cellulo* model level but also in animal models of zebrafish and mice.

This study is the first thorough evaluation of the potential biological impact of PNMVA polymers for post-insertion modification of lipoplexes for siRNA delivery. All these observations emphasize that

Published in : Advanced Healthcare Materials (2024), vol. 13, n°08, pp. 2302712
DOI: 10.1002/adhm.202302712
Status : Postprint (Author's version)

DSPE-PNMVA$_{24}$ is a promising alternative to DSPE-PEG, with comparable stealth and toxicity properties but with the advantages of guaranteeing better efficacy, by minimizing the *dilemma* effect, and less immunological reaction (no ABC or HSR effects).

In addition, this study demonstrates the promise of DSPEPNMVA derivatives for successful use in LNP formulations, which are now commonly used to deliver nucleic acids. The transferability to LNP formulation was demonstrated as PNMVA-decorated LNPs showed similar stealth properties with high efficiency in tumor cells, even in serum containing medium, which considerably broadens the scope of PNMVA derivatives for siRNA delivery.

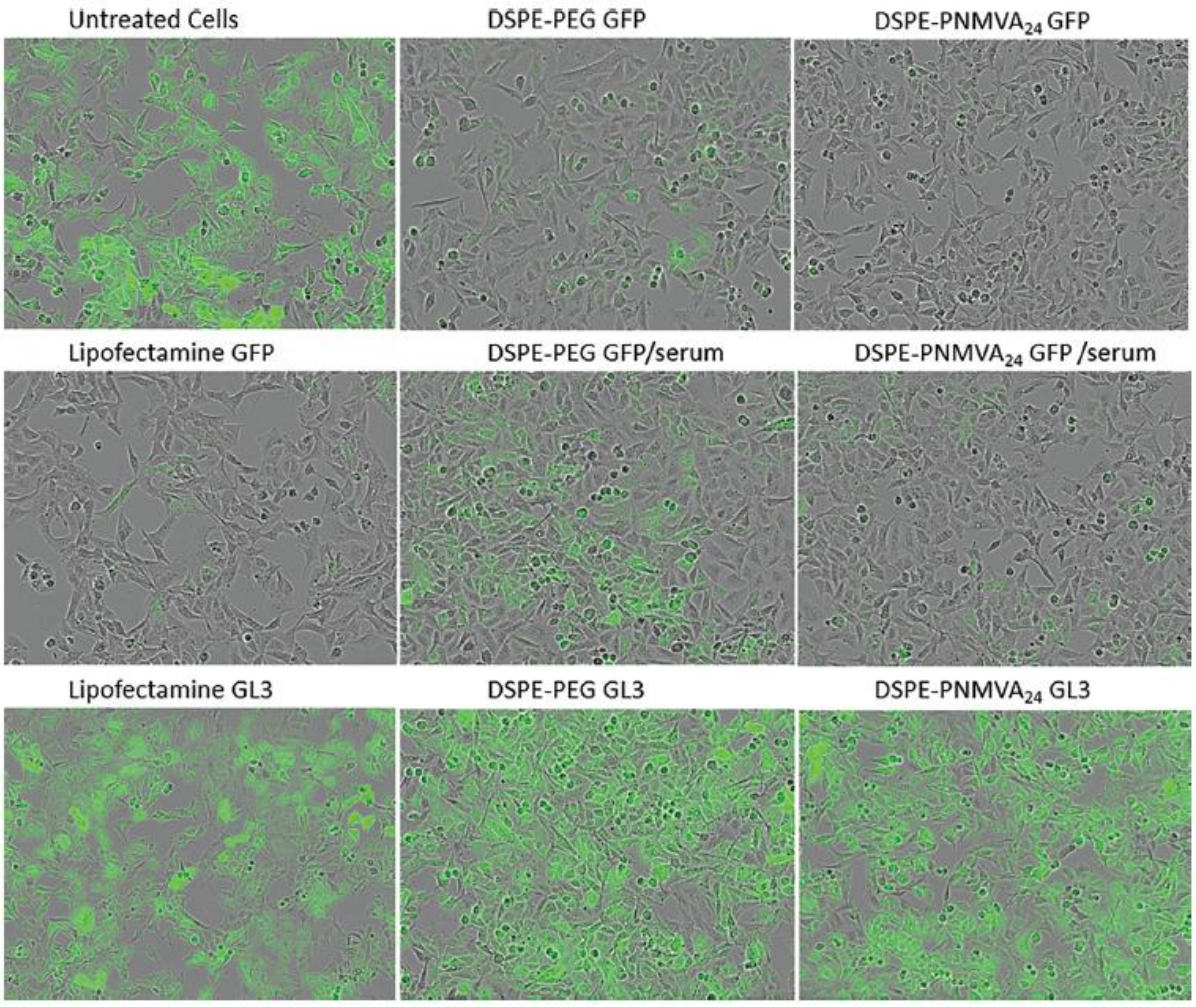

Figure 13. Representative composite phase contrast and fluorescent pictures of A549/GFP cells transfected with Lipofectamine, LNPs including DSPEPEG or DSPE-PNMVA24, in serum-free or serum-containing medium, 72 h after transfection. Lipofectamine and LNPs were prepared with siGFP or siGL3 and diluted to obtain a final concentration of 100 nm.

Overall, decorating lipid-nanocarriers with PNMVA instead of PEG or PNVP opens brand new perspectives in the field of siRNA delivery and should contribute to improve the safety and efficiency of future nanocarriers.[54]

Published in : Advanced Healthcare Materials (2024), vol. 13, n°08, pp. 2302712
DOI: 10.1002/adhm.202302712
Status : Postprint (Author's version)

4. Experimental Section

Polymer Synthesis: The detailed synthesis and characterization of the PNMVA derivatives (Et-PNMVA, OD-PNMVA and DSPE-PNMVA) are provided in the supporting information section (**Scheme S1, Tables S1–S3, Figures S1–S3, Supporting Information**).

Membrane Interaction: QCM-D analyses of the polymer/membrane interactions were carried out following a procedure described elsewhere.[35] Deposition of the DOTAP/Chol/DOPE membrane onto the gold coated sensors (Q-Sense AT-cut quartz crystal sensors, fundamental frequency of 5 MHz) described in ref.[35] was inspired from a membrane deposition method reported by Martin et al.[45,46] The sensor modified by the DOTAP/Chol/DOPE membrane was then exposed to solutions of the different PNMVA derivatives (30 µm in high salt PBS buffer).

Preparation of Liposome and Lipoplex Formulations: Cationic liposomes, lipoplexes, and post-grafted lipoplexes were prepared as previously described.[35,55–59]

Preparation of Lipid Nanoparticles: The LNPs were prepared by a rapid mixing method as previously described.[49] CSL3, DSPC, Chol, and DSPEPEG or DSPE-PNMVA$_{24}$ dissolved in ethanol (1 mm total lipid concentration) in a molar ratio of 50/10/37.5/2.5 (0.5 mL) were mixed with an siRNA solution (1.5 mL) prepared in PBS buffer pH 7.4 (N/P ratio of 4).

Size, PdI, and Surface Charge: The size (Z-average size (nm) and the polydispersity index (PdI) of lipoplexes and LNPs were determined by Dynamic Light Scattering (DLS) using the Malvern Zetasizer (Nano ZS, Malvern Instrument, UK) in RNAse-free water with a fixed angle of 90°. The zeta potential (ζ) was determined with the same instrument.

Complexation Efficiency: The uncomplexed siRNA was quantified using a Quant-it RiboGreen RNA assay (Invitrogen (ThermoFisher Scientific, Walthman, MA, USA)) according to the manufacturer's instructions and as previously described.[35,49]

Protein Corona Formation: The protein corona formation around lipoplexes and LNPs was evaluated by NTA as previously described.[35,49]

Cell Culture: Human lung adenocarcinoma cells A549, obtained from the American Type Culture Collection (ATCC, University Blvd, Manassas, VA, USA), and A549/GFP cells were maintained in Dulbecco's modified Eagle medium (DMEM) (Biowest, VWR, Leuven, Belgium) supplemented with 10% FBS and 1% of PenStrep (Gibco (Invitrogen, ThermoFisher Scientific, Walthman, MA, USA)) at 37 °C in 5% CO_2-humidified atmosphere.

Cell Viability Assay: A549 cells were seeded in 96-well plates (5×10^3 cells well^{-1}). After 24 h, cells were incubated for 4 h with lipoplexes (100 nm siGL3) prepared in Opti-MEM (Gibco (Invitrogen, ThermoFisher Scientific, Walthman, MA, USA)). Then, the formulations were replaced by fresh culture medium for 20 h. 10% (v/v) MTT (3-(4,5-Dimethylthiazol2-yere)−2,5-Diphenyltetrazolium Bromide) reagent (Invitrogen by ThermoFisher Scientific, Bleiswijk, Netherlands) were added to cells and incubated for 3 h at 37 °C. Non-treated cells were used as negative control and cells treated with hydrogen peroxide solution (H_2O_2, Sigma Aldrich Chimie GmbH) at 20 mm were used as positive control. The absorbance was measured at 450 nm using MikroWin 2010 software (Labsis Laborsysteme GmbH, Neunkirchen-Seelscheid, Germany) on a TriStar^{2}S LB 942 multimode reader (Berthold Technologies, Vilvoorde, Belgium).

In Vivo Acute Toxicity in Zebrafish Model: Adult zebrafish (*Danio rerio*) were maintained while fulfilling the criteria of the Ethical Committee for the Use of Laboratory Animals at the University of Liège (Protocol #212313). The assessment of lipoplex toxicity in Zebrafish was evaluated as previously described.[35]

Published in : Advanced Healthcare Materials (2024), vol. 13, n°08, pp. 2302712
DOI: 10.1002/adhm.202302712
Status : Postprint (Author's version)

Cellular Internalization: 1×10^5 A549 cells were seeded in 24-well plates. After 24 h of adhesion, cells were treated with lipoplexes prepared with 100 nm of siGL3 Cy 5 in OptiMEM and were incubated for 4 h. After incubation, cells were washed with PBS, harvested with Trypsin-EDTA and re-suspended in PBS. The intracellular fluorescence of Cy5was measured using BD FACS Canto II flow cytometer (BD Biosciences, Franklin Lakes, USA).

Gene Silencing Efficiency: The lipoplex gene silencing efficiency was evaluated as previously described[35] by measuring the fluorescence intensity of A549/GFP cells treated with lipoplexes.

Animals: All animal experiments were examined and approved by the Animal and Ethics Review Committee of the University of Liège (Protocol #21-2397). 8 weeks aged female BALB/c mice (20–25g) purchased from Janvier Labs (Saint-Berthevin, France) were used for this study. Mice were housed in a controlled environment and had free access to water and food during the experimental period. Mice were randomly divided to three groups with eight mice in each group as following: i) a PBS control group, ii) a DSPE-PEG lipoplexes group, and iii) a DSPE-PNMVA$_{24}$ lipoplexes group, injected at a concentration of 1 mg kg^{-1} of siGL3 Cy 5.5.

Biodistribution and ABC Effect: The biodistribution and ABC effect were investigated using in vivo fluorescence imagining after intravenous injection of 100 µL of grafted lipoplexes (15% DSPE-PEG and DSPEPNMVA$_{24}$ polymer) containing 1 mg kg^{-1} of siGL3 Cy 5.5 at N/P 2.5 and isotonized with mannitol, once a week for 2 weeks. 5 and 24 h after each injection images were acquired on live animals using Living Image software in IVIS Spectrum in vivo Imaging System (PerkinElmer).

Mice were sacrificed 1 week after the second injection and the main organs (liver, kidney, heart, spleen, and lung) were collected for ex vivo fluorescence imaging.

Detection of IgG and IgM Anti-PEG or anti-PNMVA Antibodies and Pro-inflammatory Cytokines: On day 7 and day 14 after the first injection, blood was collected from mice tails and by cardiac puncture, respectively. Collected blood was placed at room temperature (RT) for 30min and then centrifuged at 1000g at 4 °C for 15 min to separate serum.

The serum of the PBS group was used as a negative control. To detect PEG- or PNMVA-specific IgM and IgG antibodies in the serum, a direct ELISA procedure was employed as previously described.[35]

IL-1β and TNF-α pro-inflammatory cytokines were detected in serum collected on day 14 using commercial ELISA kits (Mouse IL-1 beta ELISA kit and Mouse TNF-alpha ELISA kit; Invitrogen, Vienna, Austria). The dosage was performed according to manufacturer's instructions.

Live Cell Imaging: A549/GFP cells were seeded into 24-well plates at a density of 2.5×10^4 cells well^{-1} 24 h before transfection. Then, culture medium was replaced by 0.3 mL of Opti-MEM containing LNPs (100 nm of siGFP or siGL3) or LNPs supplemented with 10% FBS for 4 h, and the transfection medium was replaced by fresh culture medium. Cell population images were obtained over time using an IncuCyte SX5 live cell imaging system (Sartorius, Göttingen, Germany) as previously described.[49] The phase contrast and fluorescence images were acquired over time for 72 h. For each experiment (n = 3), the fluorescence intensity of each cell measured at 72 h was used to calculate a population median value for each formulation tested. These median values were then used to quantify the inhibition of fluorescence intensity relative to untreated cells. After 72 h of transfection, cell metabolic activity was determined using a Resazurin reduction assay (Resazurin sodium salt, Sigma-Aldrich, St. Louis, MO, USA). 90 µL of Resazurin was added to untreated cells and each well containing cells transfected with siGL3 LNPs and, after 2 h of incubation at 37 °C, 100 µL of each condition was added in triplicate into a 96-well plate. The fluorescence was measured using the Flexstation 3 Multi-Mode Microplate Reader (Molecular Devices, San Jose, CA, USA). The wavelengths of excitation and emission were 560 and 590 nm, respectively. Triton X-100 was used as a cytotoxic positive control.

Statistics: Values were expressed as means ± standard deviations (SD) for at least n = 3. PRISM (GraphPad Prism 9) was used for statistical analysis. Data were compared among groups using ANOVA

Published in : Advanced Healthcare Materials (2024), vol. 13, n°08, pp. 2302712
DOI: 10.1002/adhm.202302712
Status : Postprint (Author's version)

test followed by the Tukey' or Dunnett' multiple comparisons test depending on the method. The difference between groups was considered significant when the *p*-value was <0.05 (*), <0.01 (**), <0.001 (***), or <0.0001 (****).

Supporting Information

Materials.

1,2 distearoylphosphatidylethanolamine (DSPE)(Aldrich), magnesium sulfate (Abcr), ammonium chloride (Aldrich), lauroyl peroxide (Fluka), 2,2'-azobis(4-methoxy-2,4-dimethylvaleronitrile) (V70, t½ = 10 h at 30 °C) (Wako), hydrochloric acid (Acros), sodium phosphate monobasic monohydrate (Aldrich), sodium phosphate dibasic heptahydrate (Aldrich), sodium chloride (VWR), 1,2-dioleoyl-3-trimethylammonium-propane chloride salt (DOTAP) (Avanti polar lipids), 1,2-dioleoyl-sn-glycero-3-phosphoethanolamine (DOPE) (Avanti polar lipids), cholesterol (Aldrich), ammonium peroxide (Aldrich), 3-mercaptopropionic acid (MPA) (Aldrich), hydrogen peroxide (30%, Aldrich), sulfuric acid (95-97%, Merck), silica gel for column chromatography (60 Å, ROCC S.A.), triethylamine (99%, Acros organic), n-hexane (> 99%, VWR), ethyl acetate (≥ 99.9%, VWR), acetonitrile (≥ 99.99 %, Fisher), acetone (Fisher) and isopropanol (Fisher) were used as received. N-methyl-N-vinylacetamide (Aldrich) was dried over calcium hydride, degassed and distilled under reduced pressure prior to use. Tetrahydrofuran (THF, ≥ 99.9 %, VWR), dichloromethane (CH2Cl2, VWR) were dried over molecular sieves (4 Å) and degassed prior to use.

Ethyl-2-((ethoxycarbonothioyl)thio)propanoate (Et-XA), O-ethyl S-(1-(octadecylamino)-1-oxopropan-2-yl) carbonodithioate (OD-XA) and 2-((((2,5-dioxopyrrolidin-1-yl)oxy)carbonyl)oxy)ethyl 2-((ethoxycarbonothioyl) thio)propanoate (SC-XA) were prepared according to previously described procedures (Journal of Controlled Release, 2023, 361, 87–101). QCM-D sensors were gold coated, AT-cut quartz crystals with a fundamental frequency of about 5 MHz (Q-Sense, Sweden).

Characterization.

Size exclusion chromatography (SEC) of the polymers was carried out in DMF containing 0.025 M of LiBr at 55 °C with a Waters chromatograph equipped with two columns (PSS GRAM 100Å), a dual λ absorbance detector (Waters 2487) and a refractive index detector (Waters 2414). The system was operated at a flow rate of 1 mL/min. The molar mass of the SC-PNMVA-XA was determined by SEC equipped with a multiangle laser light scattering (MALLs) detector in DMF/LiBr (0.025 M). The Wyatt MALLs detector (120 mW solid-state laser, k 1/4 658 nm, DawnHeleos S/N342-H) measures the excess Rayleigh ratio Rh (related to the scattered intensity) at different angles for each slice of the chromatogram. The specific refractive index increment (dn/dc) of polymer was measured by using a Wyatt Optilab refractive index detector (k 1/4 658 nm). Data were processed with the Astra V software (Wyatt Technology). The system was operated at a flow rate of 1 mL/min. 1H and 13C nuclear magnetic resonance (NMR) were recorded at 298 K with a Bruker AVANCE III HD spectrometer (B0 = 9.04 T) (400 MHz) and treated with MestreNova software.

Published in : Advanced Healthcare Materials (2024), vol. 13, n°08, pp. 2302712
DOI: 10.1002/adhm.202302712
Status : Postprint (Author's version)

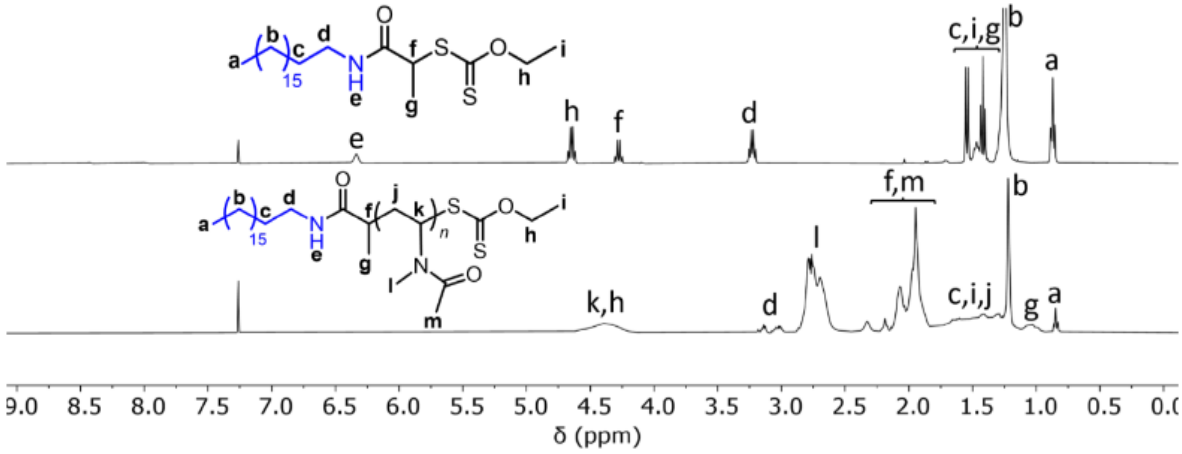

Figure S1. ^{1}H NMR spectra of OD-XA (upper spectrum) and OD-PNMVA$_{31}$ (lower spectrum).

Protocol 1. Synthesis of OD-PNMVA. OD-XA (703 mg, 1.58 mmol) and V70 (487 mg, 1.58 mmol) were placed under inert atmosphere in a Schenck tube and added with distilled, dried and degassed NMVA (7.8 g, 79 mmol). The reaction mixture was then stirred at 35 °C. After 6 h, the reaction was stopped and the monomer conversion measured by ^{1}H NMR in CD_2Cl_2 reached 50 %. The mixture was diluted in dichloromethane followed by precipitation in diethyl ether. The polymer was recovered by filtration, dried under vacuum at 40 °C for 12 h. The polymer was further purified by dialysis in acetone through a 1 kDa porous membrane for 24 h and in milliQ water through a 500 Da porous membrane for 12 h, followed by lyophilization. The desired OD- PNMVA$_{31}$ (0.98 g) was recovered as a pale yellow powder and characterized by SEC in DMF using a PS calibration ($M_{n\ SEC}$ = 1800 g/mol, Đ =1.21) and ^{1}H NMR in CD_2Cl_2 ($M_{n\ NMR\ PNMVA}$ = 3100 g/mol, DP = 31).

Published in : Advanced Healthcare Materials (2024), vol. 13, n°08, pp. 2302712
DOI: 10.1002/adhm.202302712
Status : Postprint (Author's version)

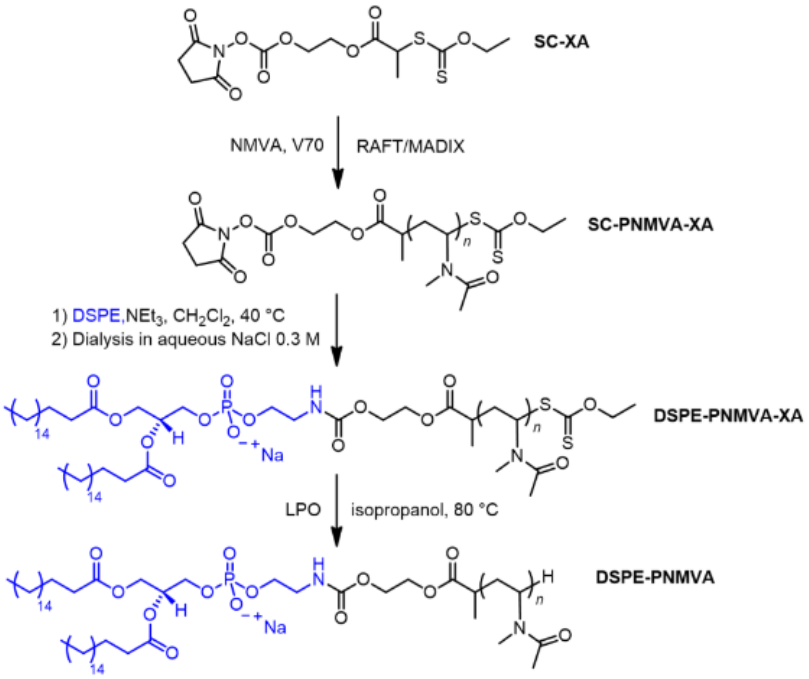

Scheme S1. General synthesis of the DSPE-PNMVA derivatives.

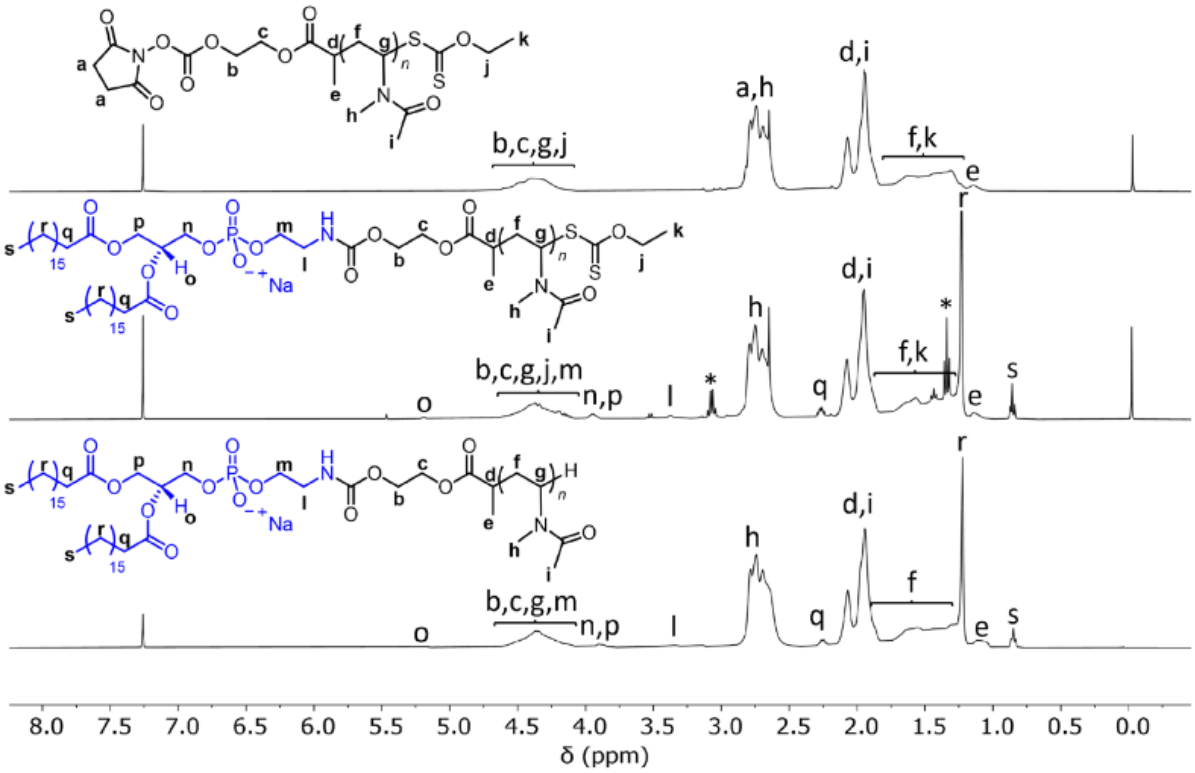

Figure S2. ^{1}H NMR spectra of DSPE-PNMVA$_{50}$ and precursors (* = residual diethyl ether).

Published in : Advanced Healthcare Materials (2024), vol. 13, n°08, pp. 2302712
DOI: 10.1002/adhm.202302712
Status : Postprint (Author's version)

Protocol 2. Synthesis of SC-PNMVA-XA. SC-XA (519 mg, 1.36 mmol) and V70 (420 mg, 1.36 mmol) were placed a under inert atmosphere in a Schenck tube and added with distilled, dried and degassed NMVA (6.8 g, 68.1 mmol). The reaction mixture was then stirred at 35 °C. After 5 h, the reaction was stopped and the monomer conversion measured by ^{1}H NMR in $CDCl_3$ reached 70 %. The mixture was diluted in dichloromethane and the polymer was purified twice by precipitation in diethyl ether. After drying under vacuum at 40 °C for 24 h, SC-PNMVA$_{40}$-XA (2.71 g) was collected as a pale yellow powder and characterized by SEC in DMF using a PS calibration ($M_{n,\,SEC}$ = 3800 g/mol, Đ = 1.20) and MALLS (dn/dc = 0.071) ($M_{n,\,MALLS}$ = 4300 g/mol, Đ = 1.16). This procedure was adapted for the production of SC-PNMVA$_{30}$-XA.

Table S1. Synthesis and characteristics of SC-PNMVA-XA.

compounds	Time (h)	Conv.[a] (%)	$M_{n,th}$[b] (g/mol)	$M_{n,\,SEC}$[c] (g/mol)	$Đ$[c]	$M_{n,\,MALLS}$[d] (g/mol)	$Đ$[d]
SC-PNMVA$_{30}$-XA	4	65	3600	3000	1.12	3400	1.17
SC-PNMVA$_{40}$-XA	6.5	70	3800	3800	1.20	4300	1.16

Conditions: $[NMVA]_0/[SC\text{-}XA]_0/[V70]_0$ = 50/1/1, 35 °C, in bulk. [a] Determined by ^{1}H NMR in $CDCl_3$ on the crude mixture by integrating the signals of the methyl group of the monomer (at 3.08 ppm, 3H) and the signals of the methyl group of the polymer (at 2.73 ppm, 3H). [b] $M_{n,\,th} = [NMVA]_0/[CTA]_0 \times conv. \times MM_{NMVA} + MM_{SC\text{-}XA}$. [c] $M_{n,\,SEC}$ determined by SEC DMF/LiBr (PS calibration) on the crude mixture. [d] Determined by MALLS in DMF/LiBr (dn/dc = 0.071 mL.g^{-1}) after purification of the polymer by precipitation two times in diethyl ether and drying under vacuum at 40 °C.

Protocol 3. Synthesis of DSPE-PNMVA-XA. SC-PNMVA$_{40}$-XA (2.0 g, 5.88 mmol), DSPE (440 mg, 5.88mmol) and triethylamine (2.5 g, 24.57 mmol) were placed in a 25 mL round-bottom flask under nitrogen atmosphere and dissolved in dried and degassed dichloromethane (10 mL). The mixture was then stirred at 40 °C for 1 h. The solvent was then evaporated and the residue dissolved in acetonitrile (12 mL) and stored at 6 °C overnight. The solution was then centrifugated two times (10 000 rpm, 15 min, 6 °C). The supernatant was collected and after solvent evaporation, the desired DSPE-PNMVA$_{53}$-XA (1.8 g) was obtained as a white powder and characterized by SEC in DMF using a PS calibration ($M_{n,\,SEC}$ = 5000 g/mol, Đ = 1.12) and ^{1}H NMR in $CDCl_3$ ($M_{n,\,NMR}$ = 5300 g/mol, DP = 53). This procedure was adapted for the production of DSPE-PNMVA$_{35}$-XA.

Published in : Advanced Healthcare Materials (2024), vol. 13, n°08, pp. 2302712
DOI: 10.1002/adhm.202302712
Status : Postprint (Author's version)

Table S2. Synthesis and characteristics of DSPE-PNMVA-XA.

Final compound	SC-PNMVA precursor	$M_{n,\,NMR}$ [a] (g/mol)	$Đ$ [b]	DP [c]
DSPE-PNMVA$_{35}$-XA	SC-PNMVA$_{30}$-XA	3400	1.12	35
DSPE-PNMVA$_{53}$-XA	SC-PNMVA$_{40}$-XA	5300	1.12	53

Conditions : $[SC\text{-}PNMVA\text{-}XA]_0/[DSPE]_0/[NEt_3]_0$ = 1/1/4.2, 40 °C, 1 h. [a] $M_{n,\,NMR}$ of PNMVA determined by ^1H NMR in $CDCl_3$ on the purified polymer based on the relative intensities of the signal of the α-terminal methyl groups (at 0.87 ppm, 6H) and the methyl signal of PNMVA (2.5- 2.9 ppm, 3H). [b] Determined by SEC DMF/LiBr (PS calibration) after purification of the polymer by dissolution in acetonitrile, centrifugation and solvent evaporation. [c] Degree of polymerization of the PNMVA segment deduced from the $M_{n,\,NMR}$.

Protocol 4. Synthesis of DSPE-PNMVA-H by removal of the terminal xanthate. The above mentioned DSPE-PNMVA$_{53}$-XA (1.2 g, 0.2 mmol) and LPO (33.5 mg, 0.084 mmol) were placed under inert atmosphere in a 10 mL round-bottom flask and dissolved in degassed isopropanol (5 mL). The mixture was then stirred at 80 °C for 8 h, a period during which LPO portions (16.8 mg, 0.042 mmol) were added every 2 h. The mixture was stirred for at 80 °C for an additional 16 h. The polymer was recovered by precipitation in *n*-hexane, dried under vacuum at 40 °C for 12 h and dialyzed through a 1 kDa porous membrane sequentially against an aqueous sodium chloride solution (0.3 M) for 12 h and against water for 12 h. After lyophilization, the desired DSPE- PNMVA$_{50}$-H was collected as a white powder (480 mg). The absence of the xanthate was confirmed by SEC-UV by the disappearance of the xanthate's characteristic absorption signal at 290 nm (**Figure S3**). This procedure was also applied to DSPE-PNMVA$_{35}$-XA leading to DSPE- PNMVA$_{24}$-H (**Table S3**).

Table S3. Characteristics of DSPE-PNMVA after removal of the terminal xanthate.

Final compound	DSPE-PNMVA-XA precursor	$M_{n,\,SEC}$ [a] (g/mol)	$Đ$ [a]	$M_{n,\,NMR}$ [b] (g/mol)	DP [c]
DSPE-PNMVA$_{50}$-H	DSPE-PNMVA$_{53}$-XA	2800	1.27	5000	50
DSPE-PNMVA$_{24}$-H	DSPE-PNMVA$_{35}$-XA	1800	1.28	2400	24

Conditions : $[DSPE\text{-}PNMVA\text{-}XA]_0/[LPO]_0$ = 1/1.2, 80 °C in isopropanol, 24 h. [a] Determined by SEC DMF/LiBr (PS calibration) after purification of the polymer by precipitation in *n*-hexane and successive dialysis in water and 0.3 M NaCl. [c] $M_{n,\,NMR}$ of PNMVA determined by ^1H NMR in $CDCl_3$ on the purified polymer based on the relative intensities of the signal of the α-terminal methyl groups (at 0.87 ppm, 6H) and the methine signal of PNMVA (4.0-4.7 ppm, 1H). [c] Degree of polymerization of the PNMVA segment deduced from the $M_{n,\,NMR}$.

Published in : Advanced Healthcare Materials (2024), vol. 13, n°08, pp. 2302712
DOI: 10.1002/adhm.202302712
Status : Postprint (Author's version)

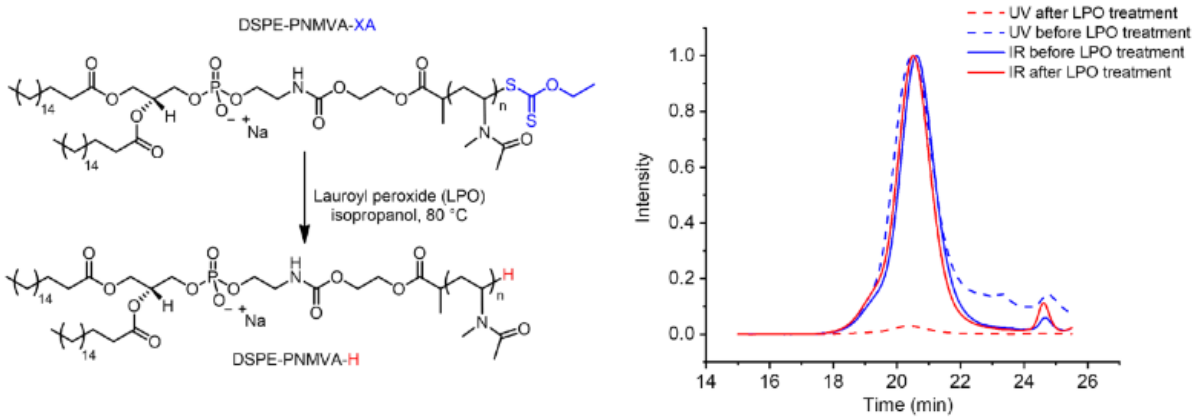

Figure S3. Overlay of the SEC-RI (solid traces) and SEC-UV (dashed traces, λ = 290 nm) of DSPE-PNMVA$_{53}$-XA before treatment with LPO (blue) and the resulting DSPE-PNMVA$_{50}$-H obtained after treatment.

Protocol 5. Synthesis of Et-PNMVA. Et-XA was synthesized according to previously reported procedures (*RSC Adv.*, **2015**, 5, 42388-42398 ; *Polymers*, **2022**, 14(4), 70). Then, Et-XA (302 mg, 1.36 mmol) and V70 (420 mg, 1.36 mmol) were placed under inert atmosphere in a Schenck tube and added with distilled and degassed NMVA (6.75 g, 68.1 mmol). The reaction mixture was then stirred at 35 °C. After 5 h, the monomer conversion measured by ^{1}H NMR in CD_2Cl_2 reached 37 %. The mixture was diluted in dichloromethane followed by two precipitations in diethyl ether. The polymer was recovered by centrifugation (1000 rpm, 6°C, 10 min) and dried under vacuum at 40 °C for 12 h. The polymer was further purified by dialysis in milliQ water through a 500 Da porous membrane for 24 h followed by lyophilization. The desired Et-PNMVA$_{27}$-XA (434 mg) was recovered as a pale yellow powder and characterized by SEC in DMF using a PS calibration ($M_{n,\,SEC}$ = 7800 g/mol, Đ = 1.23) and ^{1}H NMR in CD_2Cl_2 ($M_{n,\,NMR\ PNMVA}$ = 2700 g/mol , DP = 27).

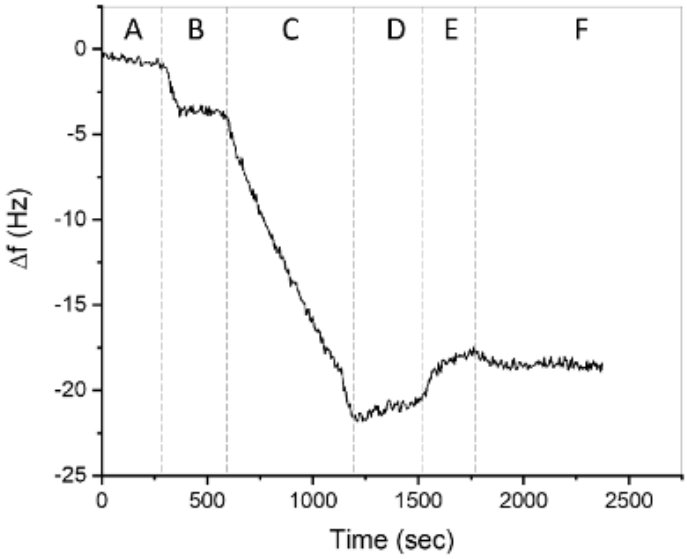

Figure S4. Typical QCM traces for the deposition of a DOTAP/Chol/DOPE (44.44%/33.33%/22.22%) membrane at 25 °C (7th harmonic): **A** = water baseline (300 µL/min), **B**-**D**-**F**: High salt BPS buffer baselines (300 µL/min), **C**: Liposomes introduction (50 µL/min), **E**: Low salt PBS buffer for liposome rupture (300 µL/min).

Published in : Advanced Healthcare Materials (2024), vol. 13, n°08, pp. 2302712
DOI: 10.1002/adhm.202302712
Status : Postprint (Author's version)

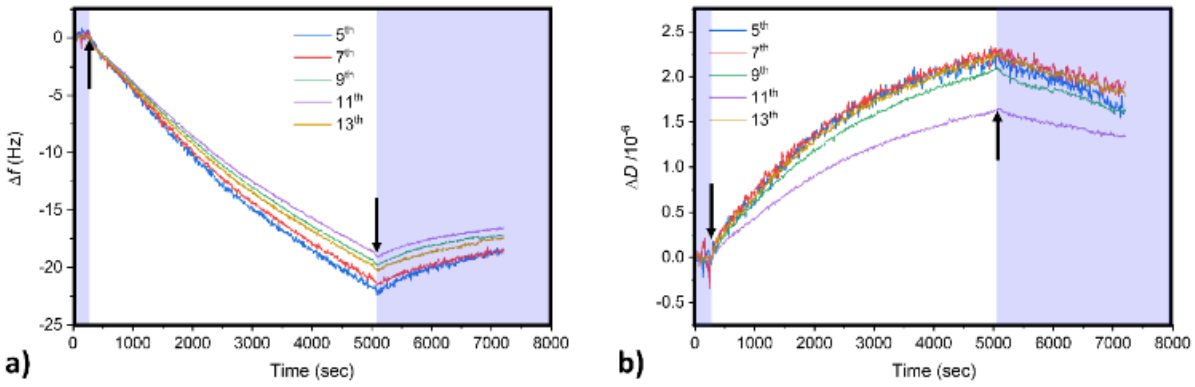

Figure S5. *Δf* (a) and *ΔD* (b) traces from QCM-D monitoring of interaction of 30 µM DSPE-PNMVA$_{24}$ with a DOTAP/Chol/DOPE(44.44%/33.33%/22.22%) membrane at 25 °C at different harmonics. Arrows designate the polymer solution addition and the final rising with buffer. Blue regions correspond to buffer elution periods.

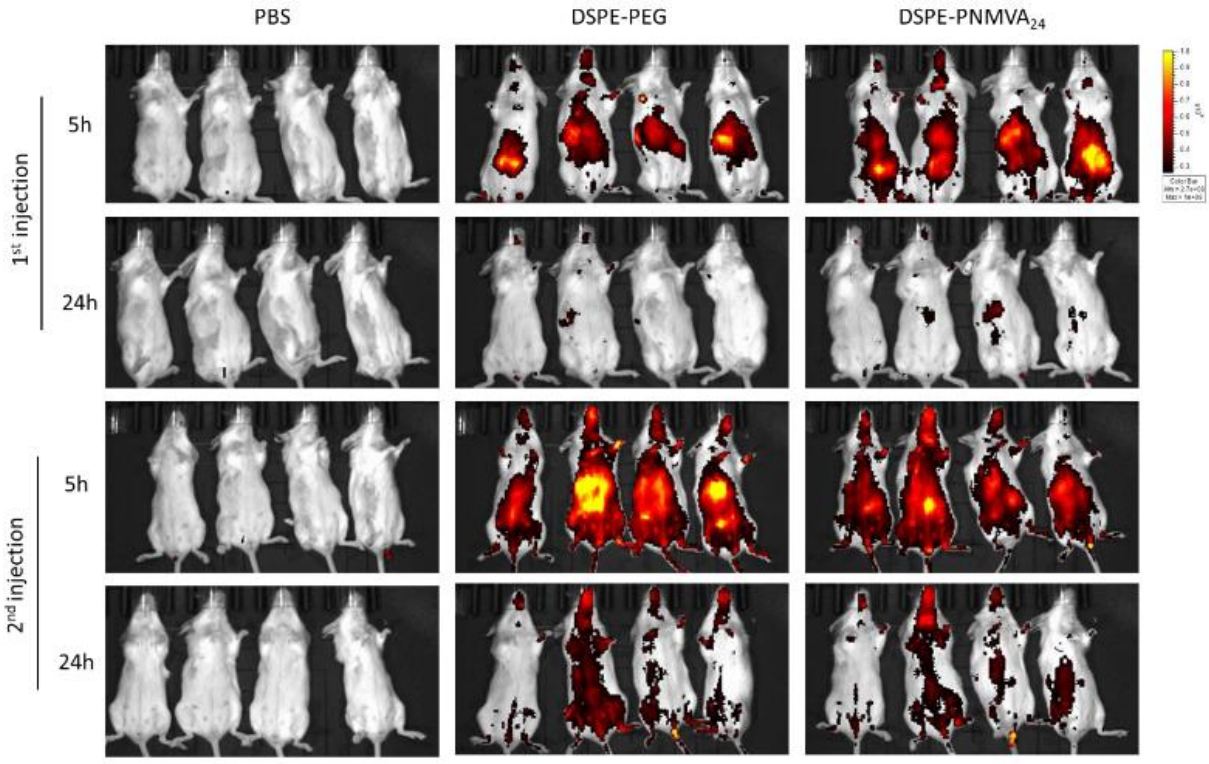

Figure S6. Mouse whole-body biodistribution imaging of DSPE-PEG and DSPE-PNMVA$_{24}$ grafted-lipoplexes and PBS injected mice after 5h and 24h of the first and the second injection.

Published in : Advanced Healthcare Materials (2024), vol. 13, n°08, pp. 2302712
DOI: 10.1002/adhm.202302712
Status : Postprint (Author's version)

Acknowledgements

M.B., F.T., and S.B.D. are co-first authors. D.M., A.D., and G.P. are co-last authors. The research was supported by the Wallonia-Brussels Federation (grant for Concerted Research Actions, LIPEGALT project, ULiège). Authors would like to thank Luc Duwez and Olivier Nivelles (GIGA-Mouse facility, University of Liege) for their help in mice experiments. The author's data of flow cytometry and toxicity in Zebrafish were obtained with the assistance of the GIGA-Flow Cytometry and GIGA-Zebrafish facilities of the University of Liege. A.D. and D.M. are FNRS Senior Research Associate. They thank FNRS for financial support.

Conflict of Interest

The authors declare no conflict of interest.

Data availability Statement

The data that support the findings of this study are available from the corresponding author upon reasonable request.

Published in : Advanced Healthcare Materials (2024), vol. 13, n°08, pp. 2302712
DOI: 10.1002/adhm.202302712
Status : Postprint (Author's version)

[1] C. H. Albertsen, J. A. Kulkarni, D. Witzigmann, M. Lind, K. Petersson, J. B. Simonsen, *Adv. Drug Delivery Rev.* **2022**, *188*, 114416.
[2] F. P. Polack, S. J. Thomas, N. Kitchin, J. Absalon, A. Gurtman, S. Lockhart, J. L. Perez, G. Pérez Marc, E. D. Moreira, C. Zerbini, R. Bailey, K. A. Swanson, S. Roychoudhury, K. Koury, P. Li, W. V. Kalina, D. Cooper, R. W. Frenck Jr, L. L. Hammitt, O. Tureci, H. Nell, A. Schaefer, S. Unal, D. B. Tresnan, S. Mather, P. R. Dormitzer, U. Sahin, K. U. Jansen, W. C. Gruber, *N. Engl. J. Med.* **2020**, *383*, 2603.
[3] D. Adams, A. Gonzalez-Duarte, W. D. O'Riordan, C.-C. Yang, M. Ueda, A. V. Kristen, I. Tournev, H. H. Schmidt, T. Coelho, J. L. Berk, K.-P. Lin, G. Vita, S. Attarian, V. Polante-Bordeneuve, M. M. Mezei, J. M. Campistol, J. Buades, T. H. Brannagam 3rd, B. J. Kim, J. Oh, Y. Parman, Y. Sekijima, P. N. Hawkins, S. D. Solomon, M. Polydefkis, P. J. Dyck, P. J. Gandhi, S. Goyal, J. Chen, A. L. Strahs, et al., *N. Engl. J. Med.* **2018**, *379*, 11.
[4] L. R. Baden, H. M. El Sahly, B. Essink, K. Kotloff, S. Frey, R. Novak, D. Diemert, S. A. Spector, N. Rouphael, C. B. Creech, J. Mcgettigan, S. Khetan, N. Segall, J. Solis, A. Brosz, C. Fierro, H. Schwartz, K. Neuzil, L. Corey, P. Gilbert, H. Janes, D. Follmann, M. Marovich, J. Mascola, L. Polakowski, J. Ledgerwood, B. S. Graham, H. Bennett, R. Pajon, C. Knightly, et al., *N. Engl. J. Med.* **2021**, *384*, 403.
[5] J. Rüger, S. Ioannou, D. Castanotto, C. A. Stein, *Trends Pharmacol. Sci.* **2020**, *41*, 27.
[6] T. Thanh, H. Thi, E. J. A. Suys, J. S. Lee, D. H. Nguyen, K. D. Park, N. P. Truong, *Vaccines* **2021**, *8*, 359.
[7] Y. Sakurai, H. Hatakeyama, Y. Sato, M. Hyodo, H. Akita, H. Harashima, *Mol. Ther.* **2013**, *21*, 1195.
[8] J. S. Suk, Q. Xu, N. Kim, J. Hanes, L. M. Ensign, *Adv. Drug Delivery Rev.* **2016**, *99*, 28.
[9] Q. Yang, S. K. Lai, *Wiley Interdiscip. Rev. Nanomed. Nanobiotechnol.* **2015**, *7*, 655.
[10] T. Ishida, M. Harada, X. Y. Wang, M. Ichihara, K. Irimura, H. Kiwada, *J. Controlled Release* **2005**, *105*, 305.
[11] A. S. Abu Lila, H. Kiwada, T. Ishida, *J. Controlled Release* **2013**, *172*, 38.
[12] A. S. Nosova, O. O. Koloskova, A. A. Nikonova, V. A. Simonova, V. V. Smirnov, D. Kudlay, M. R. Khaitov, *MedChemComm* **2019**, *10*, 369.
[13] F. Zahednezhad, M. Saadat, H. Valizadeh, P. Zakeri-Milani, B. Baradaran, *J. Controlled Release* **2019**, *305*, 194.
[14] T. Suzuki, Y. Suzuki, T. Hihara, K. Kubara, K. Kondo, K. Hyodo, K. Yamazaki, T. Ishida, H. Ishihara, *Int. J. Pharm.* **2020**, *588*, 119792.
[15] S. Zalba, T. L. M. Ten Hagen, C. Burgui, M. J. Garrido, *J. Controlled Release* **2022**, *351*, 22.
[16] A. A. D'souza, R. Shegokar, *Expert Opin. Drug Deliv.* **2016**, *13*, 1257.
[17] H. Hatakeyama, H. Akita, H. Harashima, *Biol. Pharm. Bull.* **2013**, *36*, 892.
[18] D. Vllasaliu, R. Fowler, S. Stolnik, *Expert Opin. Drug Deliv.* **2014**, *11*, 139.
[19] Y. Xia, J. Tian, X. Chen, *Biomaterials* **2016**, *79*, 56.
[20] M. Kanamala, B. D. Palmer, H. Ghandehari, W. R. Wilson, Z. Wu, *Pharm. Res.* **2018**, *35*, 154.
[21] M. Dominska, D. M. Dykxhoorn, *J. Cell Sci.* **2010**, *123*, 1183.
[22] Y. Luo, Y. Hong, L. Shen, F. Wu, X. Lin, *AAPS PharmSciTech* **2021**, *22*, 34.
[23] J. Kopecek, J. Yang, *Adv. Drug Delivery Rev.* **2020**, *156*, 40.
[24] M. Kurakula, G. S. N. K. Rao, *J. Drug Delivery Sci. Technol.* **2020**, *60*, 102046.
[25] M. Kurakula, G. S. N. Koteswara Rao, *Eur. Polym. J.* **2020**, *136*, 109919. [26] W. B. Liechty, D. R. Kryscio, B. V. Slaughter, N. A. Peppas, *Annu. Rev. Chem. Biomol. Eng.* **2010**, *1*, 149.
[27] N. Roka, O. Kokkorogianni, P. Kontoes-Georgoudakis, I. Choinopoulos, M. Pitsikalis, *Polymers (Basel)* **2022**, *14*, 701.
[28] M. S. B. Husain, A. Gupta, B. Y. Alashwal, S. Sharma, *Energy Sources Part A* **2018**, *40*, 2388.
[29] M. Teodorescu, M. Bercea, S. Morariu, *Biotechnol. Adv.* **2019**, *37*, 109. [30] M. Teodorescu, M. Bercea, *Polym. – Plast. Technol. Eng.* **2015**, *54*, 923.
[31] V. Pautu, E. Lepeltier, A. Mellinger, J. Riou, A. Debuigne, C. Jérôme, N. Clere, C. Passirani, *Cancers* **2021**, *13*, 2028.
[32] P. H. Kierstead, H. Okochi, V. J. Venditto, T. C. Chuong, S. Kivimae, J. M. J. Fréchet, F. C. Szoka, *J. Controlled Release* **2015**, *213*, 1.
[33] V. P. Torchilin, T. S. Levchenko, K. R. Whiteman, A. A. Yaroslavov, A. M. Tsatsakis, A. K. Rizos, E. V. Michailova, M. I. Shtilman, *Biomaterials* **2001**, *22*, 3035.
[34] I. A. Yamskov, A. N. Kuskov, K. K. Babievsky, B. B. Berezin, M. A. Krayukhina, N. A. Samoylova, V. E. Tikhonov, M. I. Shtilman, *Appl. Biochem. Microbiol.* **2008**, *44*, 624.
[35] M. Berger, F. Toussaint, S. B. Djemaa, J. Laloy, H. Pendeville, B. Evrard, C. Jerôme, A. Lechanteur, D. Mottet, A. Debuigne, G. Piel, *J. Controlled Release* **2023**, *361*, 87.
[36] W. Fan, S. Yamago, *Angew. Chem., Int. Ed.* **2019**, *58*, 7113.
[37] M. Dréan, P. Guégan, C. Detrembleur, C. Jérôme, J. Rieger, A. Debuigne, *Macromolecules* **2016**, *49*, 4817.
[38] A. Debuigne, A. N. Morin, A. Kermagoret, Y. Piette, C. Detrembleur, C. Jérôme, R. Poli, *Chem. Eur. J.* **2012**, *18*, 12834.
[39] M. Dréan, A. Debuigne, C. Goncalves, C. Jérôme, P. Midoux, J. Rieger, P. Guégan, *Biomacromolecules* **2017**, *18*, 440.
[40] A. Dupre–Demorsy, O. Coutelier, M. Destarac, C. Nadal, V. Bourdon, T. Ando, H. Ajiro, *Macromolecules* **2022**, *55*, 1127.
[41] P. R. Cullis, M. J. Hope, *Mol. Ther.* **2017**, *25*, 1467.
[42] W. Viricel, S. Poirier, A. Mbarek, R. M. Derbali, G. Mayer, J. Leblond, *Nanoscale* **2017**, *9*, 31.
[43] M. Langlais, O. Coutelier, M. Destarac, *Macromolecules* **2018**, *51*, 4315.
[44] M. Destarac, C. Kalai, A. Wilczewska, L. Petit, E. Van Gramberen, S. Z. Zard, *ACS Symp. Ser.* **2006**, *944*, 564.
[45] T. John, Z. X. Voo, C. Kubeil, B. Abel, B. Graham, L. Spiccia, L. L. Martin, *MedChemComm* **2017**, *8*, 1112.
[46] A. Mechler, S. Praporski, K. Atmuri, M. Boland, F. Separovic, L. L. Martin, *Biophys. J.* **2007**, *93*, 3907.
[47] M. C. Dixon, *J. Biomol. Tech.* **2008**, *19*, 151.
[48] G. Sauerbrey, *Z. Med. Phys.* **1959**, *155*, 206.
[49] M. Berger, M. Degey, J. Leblond Chain, E. Maquoi, B. Evrard, A. Lechanteur, G. Piel, *Pharmaceutics* **2023**, *15*, 597.
[50] H.-R. Jia, Y.-X. Zhu, Q.-Y. Duan, Z. Chen, F.-G. Wu, *J. Controlled Release* **2019**, *311*, 301.
[51] K. Y. Lee, G. H. Jang, C. H. Byun, M. Jeun, P. C. Searson, K. H. Lee, *Biosci. Rep.* **2017**, *37*, BSR2010199.
[52] A. Ledoux, A. St-Gelais, E. Cieckiewicz, O. Jansen, A. Bordignon, B. Illien, N. Di Giovanni, A. Marvilliers, F. Hoareau, H. Pendeville, J. Quetin-Leclercq, M. Frédérich, *J. Nat. Prod.* **2017**, *80*, 1750.

Published in : Advanced Healthcare Materials (2024), vol. 13, n°08, pp. 2302712
DOI: 10.1002/adhm.202302712
Status : Postprint (Author's version)

[53] S. Sieber, P. Grossen, P. Uhl, P. Detampel, W. Mier, D. Witzigmann, J. Huwyler, *Nanomed. Nanotechnol. Biol. Med.* **2019**, *17*, 82.
[54] A. Debuigne, G. Piel, D. Mottet, F. Toussaint, M. Berger, S. Ben Djemaa, A. Lechanteur, *Polymer Derivatives and Their Use as Lipid Nanoparticle Modifiers* **2023**, EP23171538, 4.
[55] A. Lechanteur, T. Furst, B. Evrard, P. Delvenne, P. Hubert, G. Piel, *Int. J. Pharm.* **2015**, *483*, 268.
[56] A. Lechanteur, T. Furst, B. Evrard, P. Delvenne, G. Piel, P. Hubert, *Mol. Pharmaceutics* **2017**, *14*, 1706.
[57] T. Furst, G. R. Dakwar, E. Zagato, A. Lechanteur, K. Remaut, B. Evrard, K. Braeckmans, G. Piel, *J. Controlled Release* **2016**, *236*, 68.
[58] T. Furst, V. Bettonville, E. Farcas, A. Frere, A. Lechanteur, B. Evrard, M. Fillet, G. Piel, A.-C. Servais, *Electrophoresis* **2016**, *37*, 2685.
[59] A. Lechanteur, T. Furst, B. Evrard, P. Delvenne, P. Hubert, G. Piel, *Eur. J. Pharm. Sci.* **2016**, *93*, 493.